Two-site Modelling Considering Lateral Interactions and Adsorption Isotherms Measurement

By

Ruiyang Zhao

A thesis submitted to Johns Hopkins University in conformity with the requirements for the degree of Master of Science in Engineering

Baltimore, Maryland

May 2019

Abstract

Catalysis is one of the most important components in chemical engineering. It directly determines the production rate which further impacts the overall revenue and profit. Also, the working temperature of the catalyst makes a great difference on the energy cost of production. However, current catalytic theories do not give an accurate description of how reactant molecules adsorb to the surface of the catalyst. In this thesis, we will present several two-site models that introduce the relationship of reaction rate versus temperature versus molecular distance and discuss about how adsorption compression influences the efficiency of the catalyst. Also, we experimentally measured the physisorption, chemisorption and total adsorption isotherms for various gases on the surface of zeolite (HZSM-5) at room temperature (35 °C). The data show that physisorption dominates the total adsorption amount, and the physisorption amount has a linear relationship with gas concentration when the gas concentration is high. Meanwhile, the chemisorption does not happen for every kind of gas, especially for inert and nonpolar gases, and the chemisorption isotherms exhibit a huge similarity with the adsorption isotherms drawn from the Grand Canonical Model.

Thesis Committee

Marc D. Donohue, Professor of Chemical Engineering

Gregory L. Aranovich, Research Professor of Chemical Engineering

Acknowledgements

During these two years, I would like to give my most sincere appreciation to Dr. Marc D. Donohue who assisted me to overcome many difficulties during the research and provided useful suggestions to deepen my understanding in this topic. In the modelling part, he accurately pointed out some inner contradictions in my models and let me gradually correct my models by considering the underlying physical principles. In the experiment part, he gave me strong support on equipment procurement and suggested many points in helping us improve the accuracy of the experiments. Another person I want to show my great appreciation is Dr. Gregory Aranovich, who led me into the realm of catalytic mechanisms and instructed me on how to create models for such behavior.

In addition, I want to thank Yutian Qian, Pengfei Xie and Peikun Wang for their assistance to me in my experiments. Yutian is my teammate and we cooperated very well in using the Autochem 2920 to get our data. Pengfei Xie and Peikun Wang are experienced research scientists in the field of catalysis. At the beginning of the experiment, they taught me how to setup the whole equipment and helped us modify the procedures to ensure accuracy.

Table of Contents

List of Tables

List of Figures

1, Introduction

a) Langmuir's Adsorption Theory

Catalysis is one of the most important parts in chemical engineering. Kinetics directly determines the production rate, which further impacts the overall revenue and profit. Moreover, working temperature of the catalyst makes great difference on the cost of production since it directly determines the energy cost. Therefore, over the last century, adsorption mechanisms have been widely studied because these mechanisms are directly associated with the design of highly efficient heterogeneous catalysts[1], and many models have been developed to describe the adsorption isotherms[2]. Among all these models, Langmuir's adsorption model is the most well-known and widely-applied model for its simplicity and accuracy to fit different data. The basic assumptions for Langmuir's theory are that the surface is homogeneous and there is no lateral energy between adsorbate molecules. Also, only the monolayer coverage can be achieved even for the maximum adsorption[3]. Based on these assumptions, we can deduct the formula to represent Langmuir's adsorption isotherm for molecule A:

$$\theta_A = \frac{K_A^{Eq} p_A}{1 + K_A^{Eq} p_A} \qquad (1)$$

where θ_A is the fraction of sites covered by the adsorbate A, p_A is the partial pressure of the adsorbate A and K_A^{Eq} is the equilibrium constant for adsorption and desorption. Figure 1 shows a sample isotherm graph for Langmuir's theory.

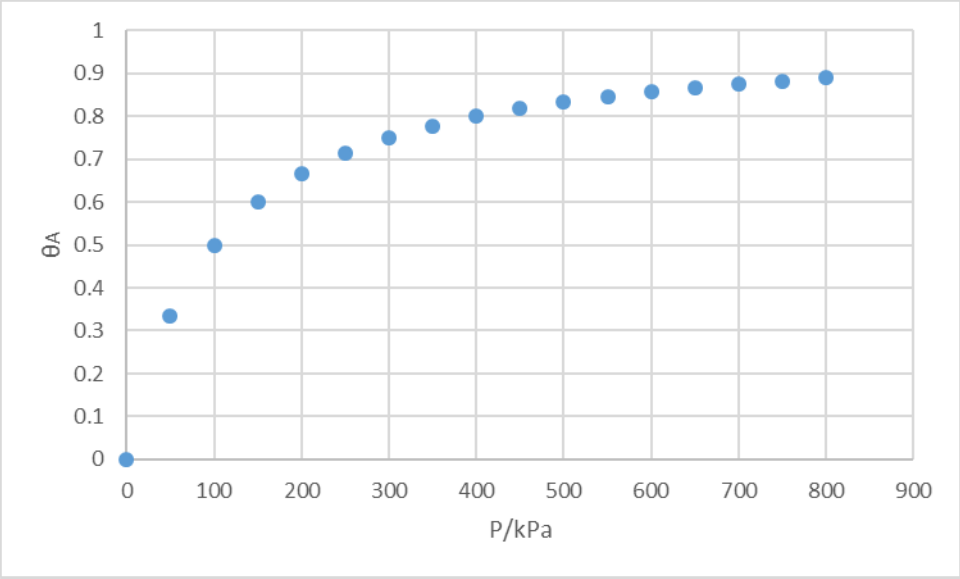

Figure 1. Langmuir's adsorption isotherm

Even though Langmuir's theory is widely used, its use is restricted by some inherent deficiencies. For example, surfaces are usually rough and inhomogeneous. Moreover, it ignores the adsorbate/adsorbate interactions. To improve Langmuir's theory, more models have been proposed since then.

b) Improved Adsorption Theory

After Langmuir proposed his theory, Frumkin[4] and Fowler and Guggenheim[5] made correction to his theory by considering the lateral interactions on the monolayer to let the theory suitable for the rough surfaces. Even though their theory can predict a two-dimensional phase transition, it neglected the interactions perpendicular to the surface[6]. In 1938, Brunauer, Emmett, and Teller[7] derived a new model for multilayer adsorption by considering adsorbate-adsorbate interactions in the direction perpendicular to the surface but did not consider the lateral interaction on the surface. As a result, the Brunauer-Emmett-Teller (BET) theory can predict multilayer behavior but cannot not deal with two-dimensional phase transitions in the absorbed layer[6].

In 1960, Ono and Kondo proposed an equation for density gradients at vaper-liquid interfaces[8]. Based on this finding, lattice density functional theory (LDFT) was developed to study fluids in a confined environment[9-12] and it has been widely applied to predict a wide variety of behavior including multiplayer adsorption[13], hysteresis in micropores[14], adsorption on surfaces with molecular-scaleheterogeneities[15], and adsorption in supercritical systems[16-18].

c) Grand Canonical Model

Grand Canonical Model is a model to describe the adsorption isotherm on the two active sites. As shown in the Figure 2, when two molecules are far from each other (case a), there is no interaction between them, and thus no reaction occurs. When the active sites are close with each other and the attraction forces between active sites and adsorbate molecules are very large, both active sites can be occupied, and the adsorbate molecules repel each (case b). When the active sites are very close with each other, one molecule will occupy both sites because the repulsive force is so big that it overcomes the attraction between an active site and the adsorbate molecule (case c).

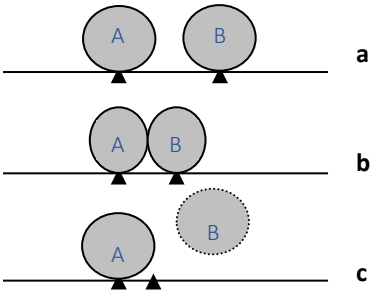

Figure 2. Molecules on active sites[6]

For the grand canonical ensemble[6], the variables are chemical potential, μ, average number of molecules on the two active sites, << N>>, and temperature, T. The grand canonical partition function for this system can be written as:

$$\Xi = \exp(-\frac{E_0}{kT}) + \exp(\frac{\mu}{kT} - \frac{E_1^{'}}{kT}) + \exp(\frac{\mu}{kT} - \frac{E_1^{''}}{kT}) + \exp(\frac{2\mu}{kT} - \frac{E_2}{kT}) \qquad (2)$$

where E_0 is the activation energy, E_1' and E_1'' are the configuration energy of only one active site is occupied, E_2 is the configuration energy of both active sites are occupied, and k is Boltzmann constant. The value of E_0, E_1', E_1'' and E_2 can be calculated by the formula below:

$$E_0 = 0 \qquad (3)$$

$$E_1' = E_1'' = \varphi_s \quad (4)$$

$$E_2 = 2\varphi_s + \varphi(d) \quad (5)$$

$\varphi(d)$ is the Lennard-Jones potential here and $\varphi(d)$ can be calculated by

$$\varphi(d) = 4*\varepsilon*[(\frac{d}{\sigma})^{-12} - (\frac{d}{\sigma})^{-6}] \quad (6)$$

, and <<N>> can be calculated by

$$<< N >> = \frac{1}{\Xi}[\exp(\frac{\mu}{kT} - \frac{E_1^{'}}{kT}) + \exp(\frac{\mu}{kT} - \frac{E_1^{''}}{kT}) + 2\exp(\frac{2\mu}{kT} - \frac{E_2}{kT})] \qquad (7)$$

Plug equation (2)-(6) into equation (7), we get

$$\ll N \gg = \frac{2\exp\left(\frac{\mu}{kT} - \frac{\varphi_s}{kT}\right) + 2\exp[\frac{\mu}{kT} - \frac{\varphi_s}{kT} - \frac{\varphi(d)}{kT}]}{1 + 2\exp\left(\frac{\mu}{kT} - \frac{\varphi_s}{kT}\right) + \exp[\frac{\mu}{kT} - \frac{\varphi_s}{kT} - \frac{\varphi(d)}{kT}]} \qquad (8)$$

2, Two-site Models Based on Grand Canonical Model

a) Inclusion of Mean Field Approximation in Arrhenius Factor of the Rate of Reaction and Adsorption Isotherm

From the Ono-Kondo isotherm[8], we have

$$x_{\mathrm{a}}(x_b) = \frac{K^* x_b}{1+K^* x_b} \qquad (9)$$

while

$$K^* = \exp\left[-\frac{\varphi_s}{kT} + \frac{z\varphi_a}{kT} x_{\mathrm{a}}(x_b)\right] \qquad (10)$$

For a bimolecular reaction, rate constant r_b can be calculated by

$$r_b = K[x_1(x_b)]^2 \qquad (11)$$

and rate constant K can be represented as

$$K = K_0 * K^* = K_0 * \exp\left[-\frac{\varphi_s}{kT} + \frac{z\varphi_a}{kT} x_{\mathrm{a}}(x_b)\right] \qquad (12)$$

Combining equation (9)-(12) together, we get the overall equation to calculate the reaction rate:

$$r_b = K_0[x_{\mathrm{a}}(x_b)]^2 exp\left[-\frac{E_0}{kT} + \frac{z\varphi_a}{kT} x_{\mathrm{a}}(x_b)\right] \qquad (13)$$

According to the definition of Arrhenius factor, then term $-\frac{E_0}{kT} + \frac{z\varphi_a}{kT} x_{\mathrm{a}}(x_b)$ should always be smaller or equal to zero. Since this model contains a lot of iteration calculations, MATLAB was used to do the calculation. Parameters and code are shown in the Appendix 2.

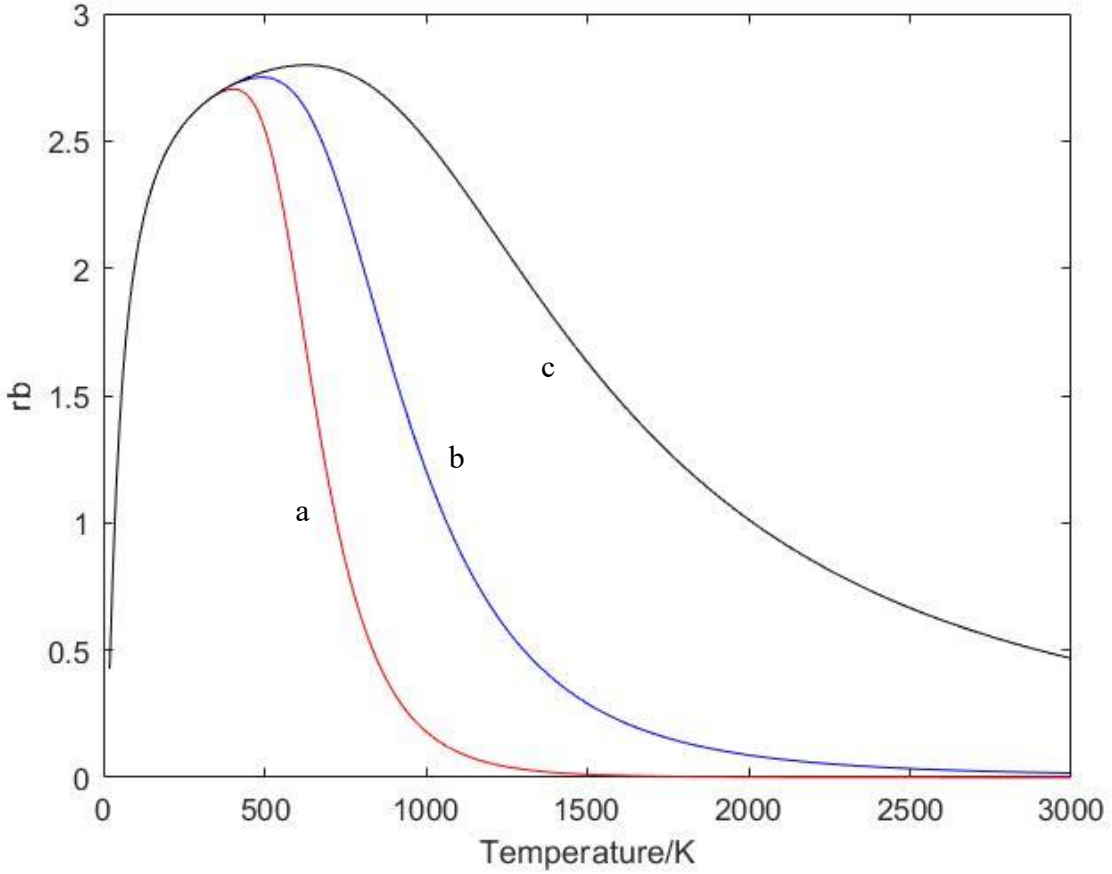

Figure 3. Reaction rate as a function of temperature at φ_s/k=-7500, ε/k=250, K_0=3, Z=1, E_0/k =2000, d/σ =0.95 and various X_b values: 0.001 (a), 0.01 (b), and 0.1 (c)

As seen from Figure 3, when the temperature goes up, the reaction rate initially increases and then gradually decreases to 0. This can be explained by the competition between adsorption and desorption. Both adsorption and desorption rates increase at higher temperature but desorption rate is more sensitive to temperature change. Since the reaction rate is the difference between adsorption and desorption, therefore there is a temperature to achieve maximum reaction rate that lower or higher temperature will slow the reaction. Another interesting phenomenon that we can get from this graph is that higher reduced density of adsorbate molecules in the bulk leads to higher reaction rate. The reason is that the higher reduced density of adsorbate molecules in the

bulk, the higher possibility that the molecules go into the interface and then the higher possibility for molecules to collide with each other, which leads to higher reaction rate.

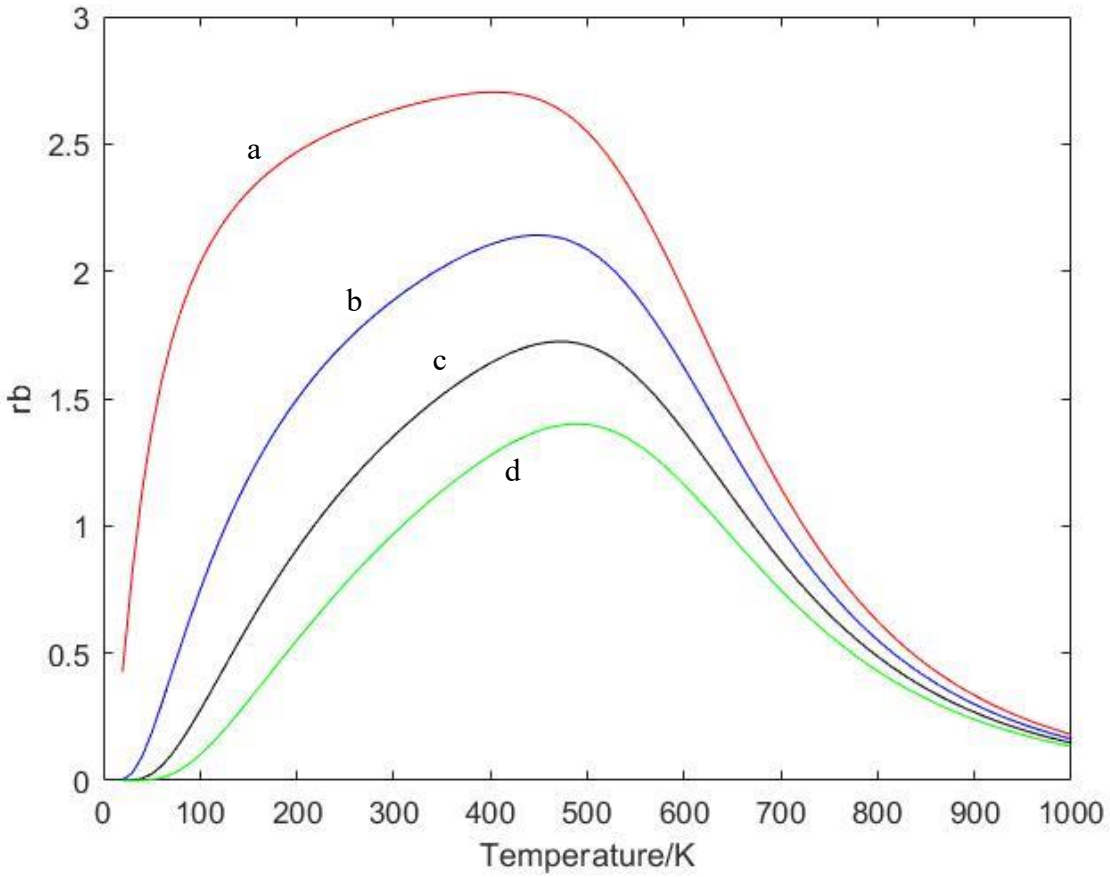

Figure 4. Reaction rate as a function of temperature at φ_s/k=-7500, ε/k=250, K_0=3, Z=1, X_b=0.001, d/σ =0.95 and various E_0/k values: 2000 (a), 2100 (b), 2200 (c), and 2300 (d)

As seen from Figure 4, higher activation energy leads to low reaction rate. The reason is that higher energy barrier decreases the percentage of the molecules that can join in the reaction according to Maxwell-Boltzmann Distribution, therefore leads to lower reaction rate.

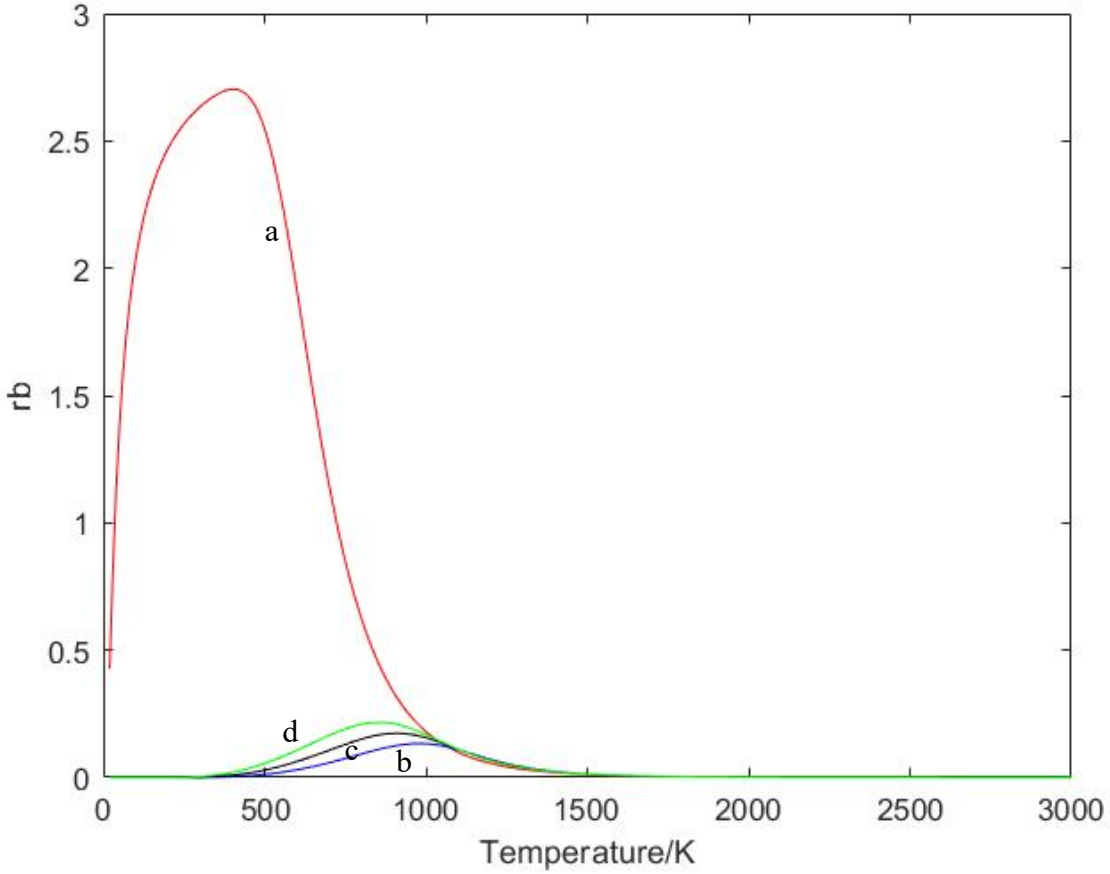

Figure 5. Reaction rate as a function of temperature at φ_s/k=-7500, ε/k=250, K_0=3, Z=1, X_b=0.001, E_0/k =2000, and various d/σ values: 0.95 (a), 1.05 (b), 1.5 (c), and 10000 (d)

As seen from Figure 5, when the distance between molecules becomes larger, the reaction rate initially decreases very fast but then gradually increases. At very far distance, the reaction still happens, which is contradictory to our assumption that only molecules that can collide with each other can join in the reaction. This graph tells us that even though this model is accurate in some ways, still some important points have been missing. Therefore, we need to develop a new model.

b) Inclusion of Non-mean Field Terms in Arrhenius Factor of the Rate of Reaction and Adsorption Isotherm

For Langmuir-Hinshelwood model, it does not consider the interaction between adsorbate molecules. In order to have a better presentation of the reaction rate, a new parameter P_{double} representing the possibility of both active sites been occupied has been incorporated to modify Langmuir-Hinshelwood model. We have the following equation

$$r_b = K_0 * P_{double} * exp\left[-\frac{E_0}{kT} + \frac{z\varphi_a}{kT} * P_{double}\right] \qquad (14)$$

The exact value of P_{double} can be calculated by

$$P_{double} = \frac{q_2}{1+q_2+2*q_1} \qquad (15)$$

From Ono-Kondo Equation, we have

$$\frac{\mu}{kT} = \ln\left(\frac{x_b}{1-x_b}\right) \qquad (16)$$

Since normally, $x_b \ll 1$, $\frac{\mu}{kT}$ can be represented as

$$\frac{\mu}{kT} = \ln\left(\frac{x_b}{1-0}\right) = \ln(x_b) \qquad (17)$$

In this way, q_1 and q_2 can be rewritten as

$$q_1 = e^{\frac{\mu}{kT} - \frac{\varphi s}{kT}} = xb * e^{-\frac{\varphi_S}{kT}} \qquad (18)$$

$$q_2 = e^{2\frac{\mu}{kT} - 2\frac{\varphi s}{kT} - \frac{\varphi_a}{kT}} = e^{2\ln(x_b) - 2\frac{\varphi_S}{kT} - \frac{\varphi_a}{kT}} = (x_b)^2 * e^{-2\frac{\varphi_S}{kT} - \frac{\varphi_a}{kT}} \qquad (19)$$

where

$$\varphi(d) = \varphi_a = 4*\varepsilon*\left[\left(\frac{d}{\sigma}\right)^{-12} - \left(\frac{d}{\sigma}\right)^{-6}\right] \qquad (6)$$

Based on the equation (6), (14), (15), (18) and (19), a model can be setup by using Mathematica to give us a clear view of the relationship between reaction rate, temperature and d/σ values. One important point here is that the factor $-\frac{E_0}{kT}+\frac{z\varphi_a}{kT} * \mathrm{P}_{\mathrm{double}}$ should always be smaller or equal to zero to remain its physical meaning. The parameters and the Mathematica code are shown on Appendix 3.

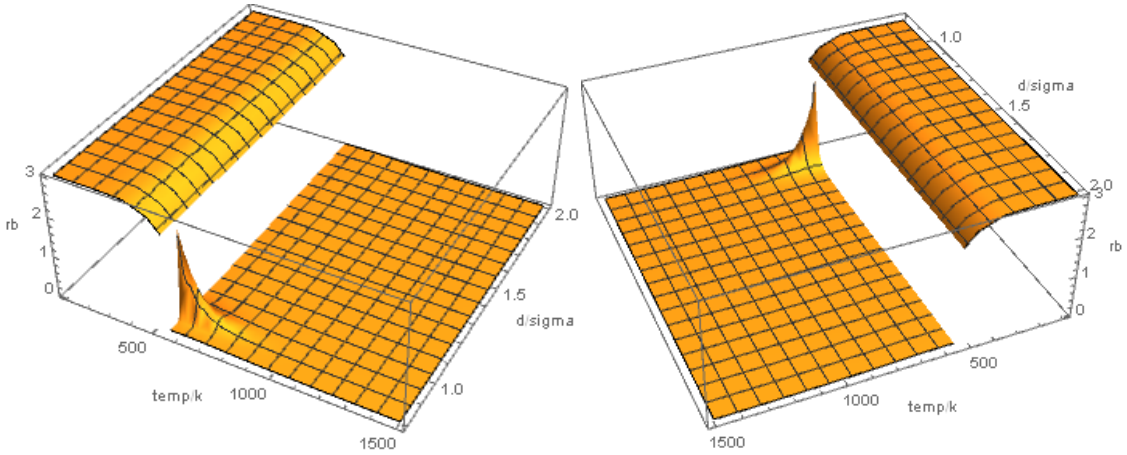

Figure 6. 3-D graph of reaction rate vs d/σ vs temperature at φ_s/k=-7500, ε/k=250, E_0/k=2000, K_0=3, Z=1, X_b=0.001

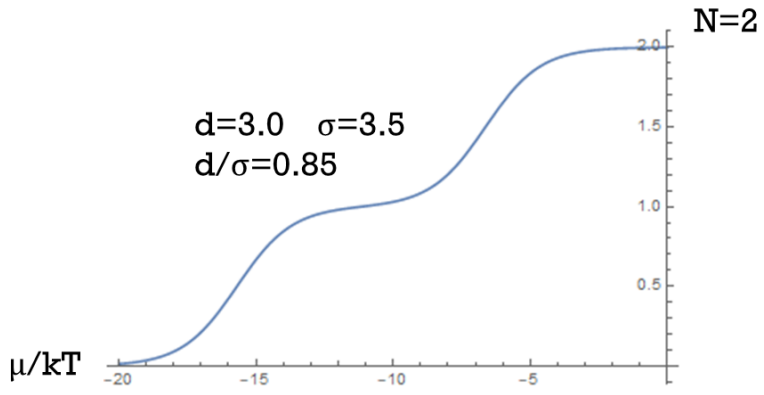

Figure 7. Adsorption isotherm of N vs μ/kT when d/σ=0.85 at φ_s/k=-7500, ε/k=250, E_0/k=2000, K_0=3, Z=1, X_b=0.001

From Figure 6 above, if we do not consider the top part, the reaction rate reaches a local maximum at around d/σ =0.85, which validates our assumption that the compression between molecules can greatly catalyze the reaction since $d/\sigma < 1$. Another interesting finding is that d/σ =0.85 is a very interesting value that coincide with the smallest distance that achieves N=2 as shown in Figure 7, which means that at this value, the compression is the largest and this potential energy greatly decreases the activation barrier for the reaction.

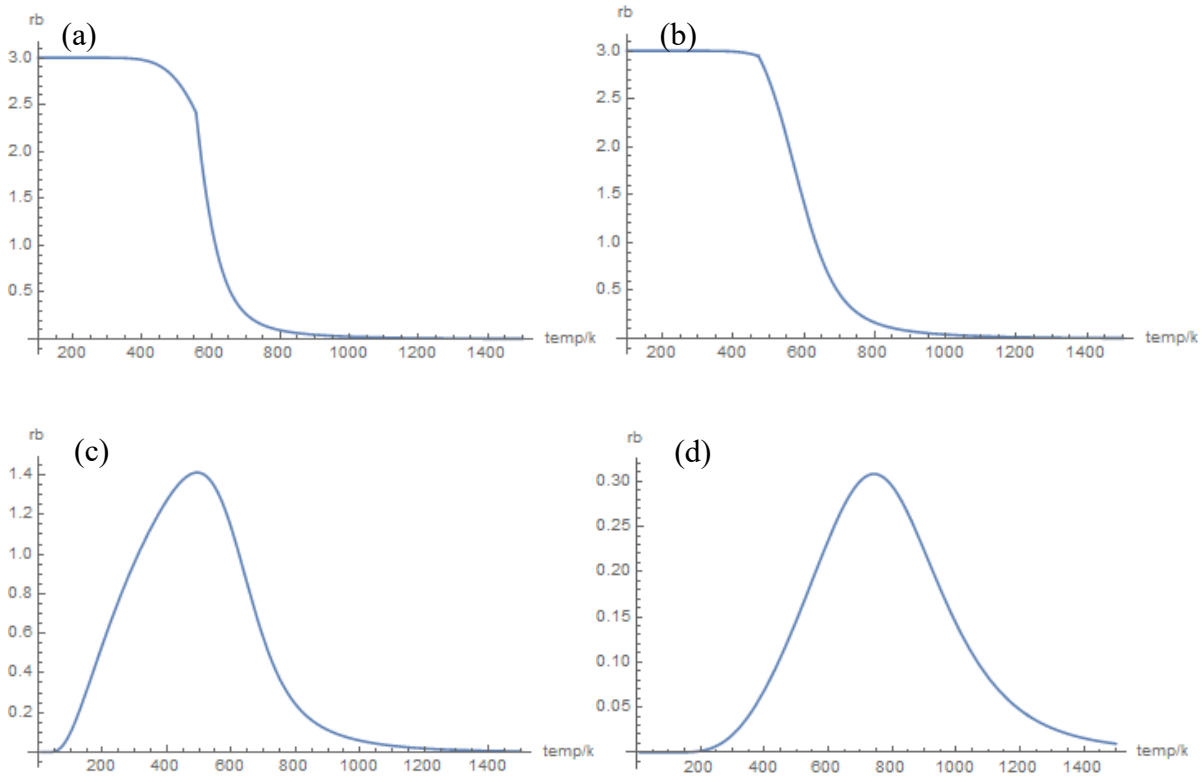

Figure 8. Graph of reaction rate vs temperature at φ_s/k=-7500, ε/k=250, E_0/k=2000, K_0=3, Z=1, X_b=0.001, and various d/σ values: 0.88 (a), 0.89 (b), 0.90 (c), and 0.95 (d)

From Figure 8, when d/σ becomes bigger, the temperature to achieve maximum reaction rate increases and the width of the curves also increases. When d/σ becomes smaller than 0.90, reaction rate initially remains stable and then decreases with temperature increases. The reason is that for small d/σ, the two molecules on the active sites are very close to each other. According

to Lennard-Jones Equation, the potential energy (repulsive force) will increase dramatically with even little decrease to the distances, which would make the two molecules bounce from each other, leading to the dramatic decrease in reaction rate. In addition, among the two competing factors that are temperature and d/σ, d/σ seems to be a more important factor in determining the magnitude of reaction rate. Therefore, the importance of d/σ in designing the catalyst that can work under the ambient temperature can be verified.

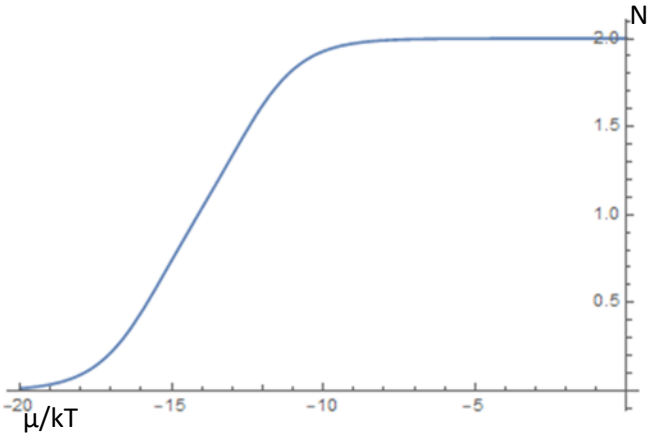

Figure 9. Graph of N vs μ/kT at φ_s/k=-7500, ε/k=250, E_0/k=2000, K_0=3, Z=1, X_b=0.001, and d/σ =0.90

Also, reaction rate begins to show a peak point at around d/σ =0.90, which means that σ/d=1.1, a very interesting value that coincide with the smallest distance that has no inflection point on the N vs μ/kT graph when N =2. As shown in Figure 9, this coincidence can be explained since the existence of the inflection point means that little energy difference makes a giant change to the number N, which changes the reaction rate abruptly since the reaction needs both sides to be occupied to happen. Thus, when the graph does not have an inflection point, the graph looks more like our ideal graph which the reaction rate initially increases and then decreases

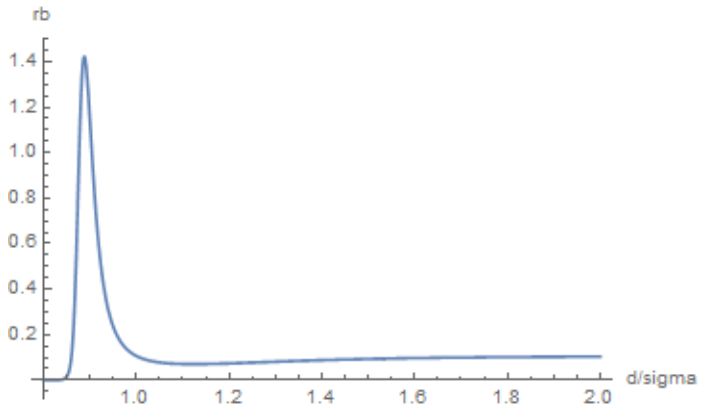

Figure 10. Reaction rate vs d/σ when T= 600K at φ_s/k=-7500, ε/k=250, E_0/k=2000, K_0=3, Z=1, X_b=0.001

As shown in Figure 10, a problem rises at low temperature that the reaction rate increases as d/σ increases when d/σ is bigger than 1.1. This phenomenon should not happen because it contradicts our assumption that the catalytic effects rise from adsorption compression. Thus, we need to consider more conditions and make correction to this model.

c) Inclusion of Collision Probability in Pre-exponential of the Rate of Reaction and Adsorption Isotherm

The main problem of the last model comes from a missing point that the actual molecules on the surface are still moving all the time instead of being static. In this way, the movement needs to be considered as it makes big effects on the collision probability. Here, parameter $P_{collision}$ is incorporated and the total equation is shown below:

$$r_b = K_0 * \mathrm{P}_{\mathrm{double}} * exp\left[-\frac{E_0}{kT} + \frac{z\varphi_a}{kT} * \mathrm{P}_{\mathrm{double}}\right] * P_{collision} \qquad (20)$$

Even though in the collision theory, people has introduced a way to calculate the collision probability, the conclusion cannot be directly used since that conclusion is based on a premise

that the particles can move freely in a three-dimensional environment. Meanwhile, the two-site model studies the special cases in one dimension and the molecules are bonded to the active sites. Thus, we cannot refer to existing work, and my deduction is shown below.

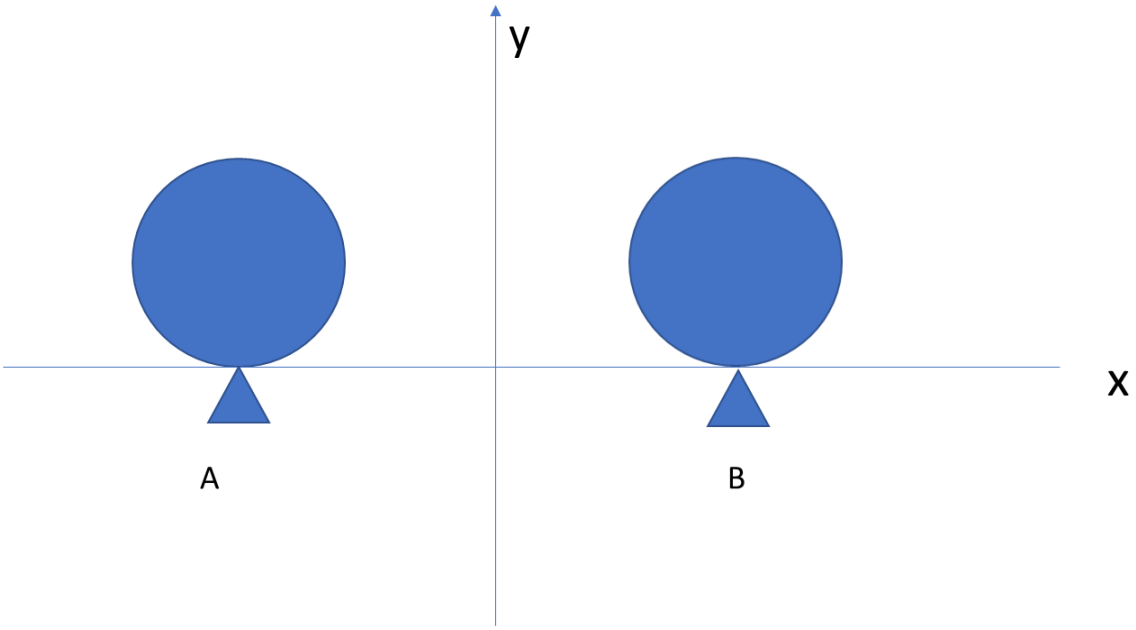

Figure 11, Illustration of molecule coordinates

As Figure 11 shows, assume both molecules can only move along x axis, and have the same kinetic energy, potential energy and movement pattern. The coordinate is $(\frac{d-\sigma}{2},0)$ for the most left point of the right ball (B). Similarly, the coordinate is $(-\frac{d-\sigma}{2},0)$ for the rightest point of the left ball (B). Assuming that the movement of both balls are simple harmonic movements with random phase differences, the position for the most left point of the right ball is $(\frac{d-\sigma}{2} + \mathrm{Asin}(\omega t),0)$ and the position for the most right point of the left ball is $(-\frac{d-\sigma}{2} + \mathrm{Asin}(\omega t + \theta),0)$ where A means the amplitude of their movements. In this way, the distance between the two points can be represented as

$$\mathrm{D} = (d - \sigma) + A[\sin(\omega t + \theta) - \sin(\omega t)] \qquad (21)$$

Since the movement speed does not affect the possibility of collision, ω is not an important factor and we can shorten our formula to

$$\mathrm{D} = (d - \sigma) + A[\sin(t + \theta) - \sin(t)] \qquad (22)$$

where $\theta \in (0, 2\pi)$. In this way, the problem becomes to find the possibility of the getting a certain value of θ that can let $\mathrm{D} \leq 0$ within a certain cycle time T. After transforming the upper equation, we get

$$[\sin(t + \theta) - \sin(t)] \geq \frac{d-\sigma}{A} = \frac{\sigma}{A}(\frac{d}{\sigma} - 1) \qquad (23)$$

Then, the main problem becomes to find the exact value of the moving amplitude of each molecule.

Assume the molecules are under ideal situation, thus the average kinetic energy for each monoatomic molecule becomes 3/2 kT. Since the total energy of each molecule on the active sites are composed of kinetic energy and potential energy, therefore the total energy is $\frac{3}{2}kT + \varphi_s + \varphi(d)$. If we set the infinitely long distance from the active site as 0 potential energy, and assume the adsorbate-adsorbent interaction as ion-dipole interaction[19], thus when the ball moves to the most distant place, the potential energy becomes $\varphi_s' = \frac{\sigma}{\sqrt{\sigma^2+4A^2}}\varphi_s$ and at this time, kinetic energy is 0. $\varphi(d)$ is negligible here because in the surfaces with strong attaction forces, its value is about two orders smaller then the sum of previous two terms.

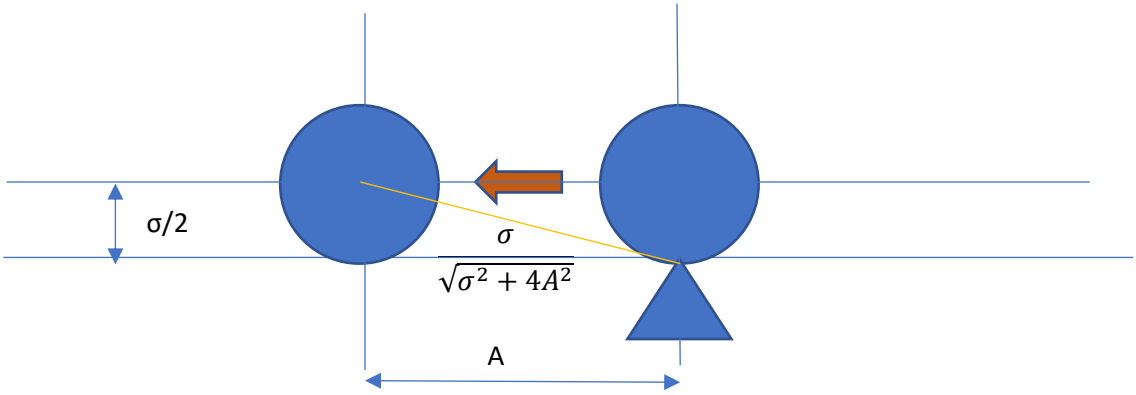

Figure 12, Maximum distance for a molecule to move

According to the law of energy conservation, for the same molecule on the active site, no matter how it moves within the range of amplitude, we have

$$\frac{3}{2}kT + \varphi_s = \varphi_s' = \frac{\sigma}{\sqrt{\sigma^2+4A^2}}\varphi_s \qquad (24)$$

After making transformation, the formula becomes

$$\frac{A}{\sigma} = \frac{\sqrt{1-(\frac{3kT}{2\varphi_s}+1)^2}}{abs(\frac{3kT}{\varphi_s}+2)} \qquad (25)$$

as both A and σ are positive.

In this way, the previous formula 1 can be rewrite into

$$\sin(t+\theta) - \sin(t) \geq \frac{abs(\frac{3kT}{\varphi_s}+2)}{\sqrt{1-(\frac{3kT}{2\varphi_s}+1)^2}}(\frac{d}{\sigma} - 1) \qquad (26)$$

To solve the inequality above, the trigonometric identities is used to transform the left side of the formula. Meanwhile, t=0 is set to minimize the number of parameters because the exact value of t does not change the result, and we have

$$\sin(\theta/2) - \sin(-\theta/2) \geq \frac{abs(\frac{3kT}{\varphi_S}+2)}{\sqrt{1-(\frac{3kT}{2\varphi_S}+1)^2}}(\frac{d}{\sigma} - 1) \qquad (27)$$

Thus, the problem of finding collision probability becomes finding the range of θ (designated as θ_{range}) within (0, 2π) that satisfy the upper inequality

$$P_{collision} = \frac{\theta_{range}}{2\pi} \quad (28)$$

In order to solve this problem consistently by the MATLAB, we did not choose to use analytical solution. Instead, we chose numeric method and picked up 1000 points evenly distributed within (0, 2π) for θ. Then, let the computer to decide whether each point satisfied the inequality. The final collision probability becomes the number of points that satisfied the inequality divided by the total number of points. The MATLAB code is attached in the Appendix 4.

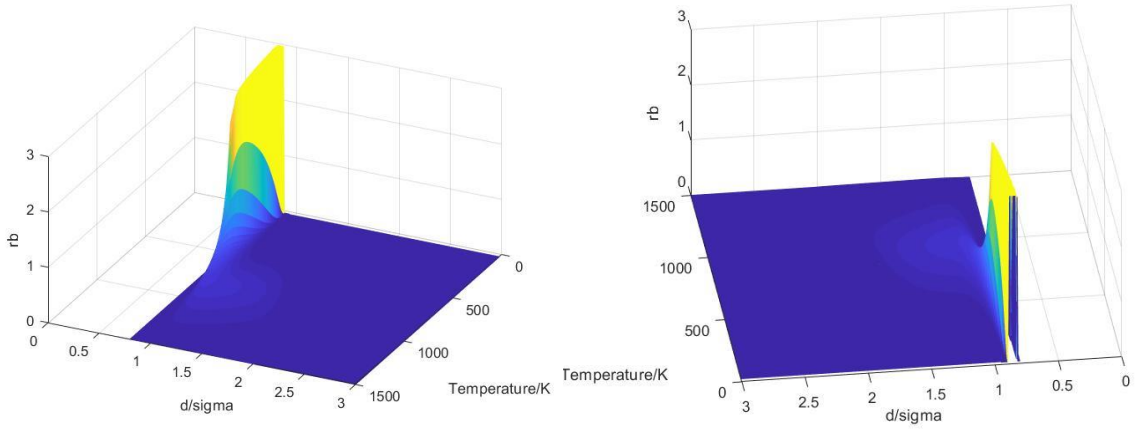

Figure 13. 3-D graph of reaction rate vs d/σ vs temperature at φ_s/k=-7500, ε/k=250, E_0/k=2000, K_0=3, Z=1, X_b=0.001

(a)

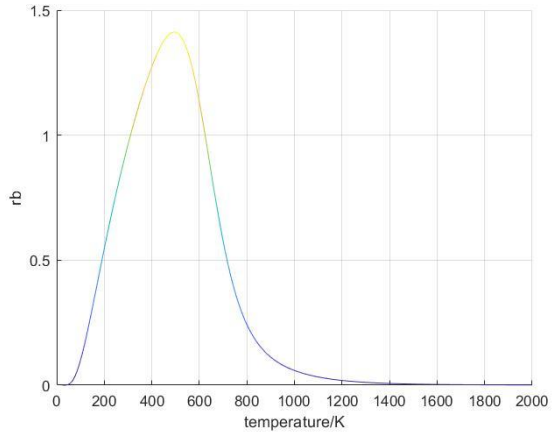

(b)

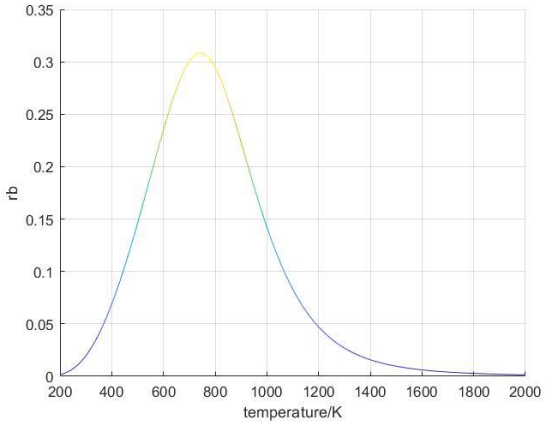

(c)

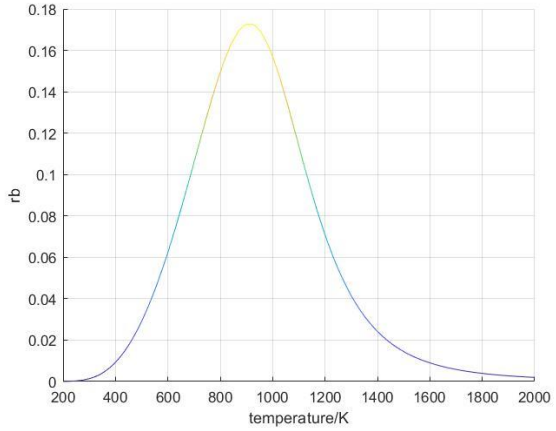

(d)

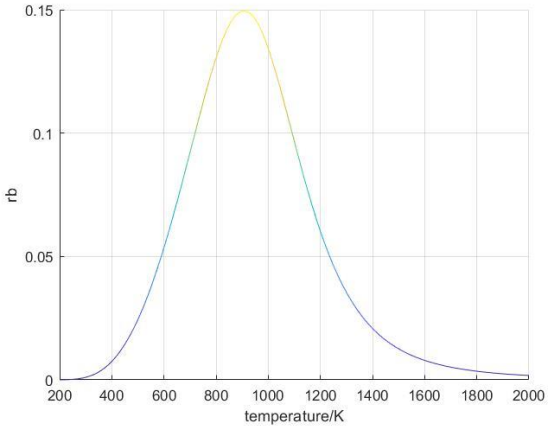

Figure 14. Graph of reaction rate vs temperature at φ_s/k=-7500, ε/k=250, E_0/k=2000, K_0=3, Z=1, X_b=0.001 and at various d/σ values: 0.90 (a), 0.95(b), 1.10 (c), and 1.25 (d)

(a)

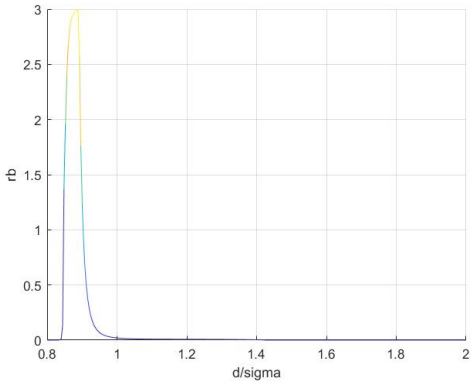

(b)

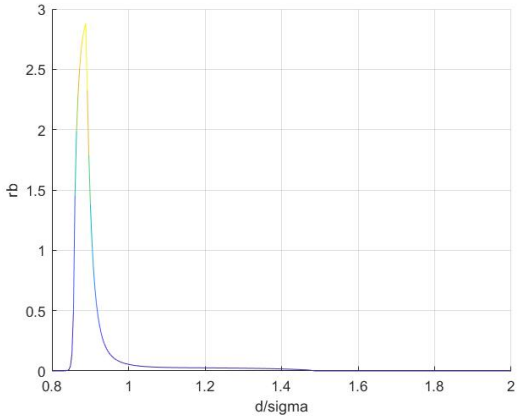

(c)

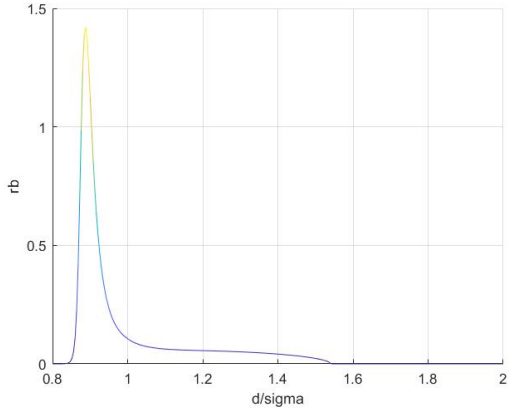

(d)

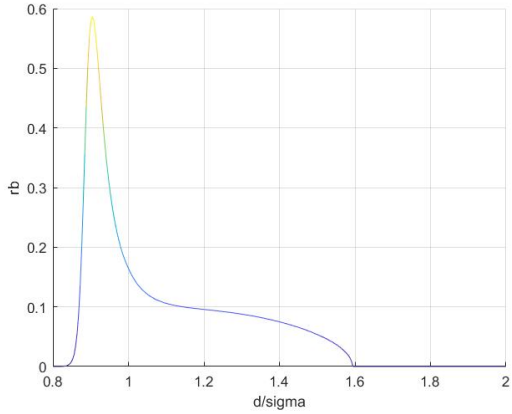

Figure 15. Graph of reaction rate vs d/σ at φ_s/k=-7500, ε/k=250, E_0/k=2000, K_0=3, Z=1, X_b=0.001 and at various T values: 400 K (a), 500 K(b), 600 K (c), and 700 K (d)

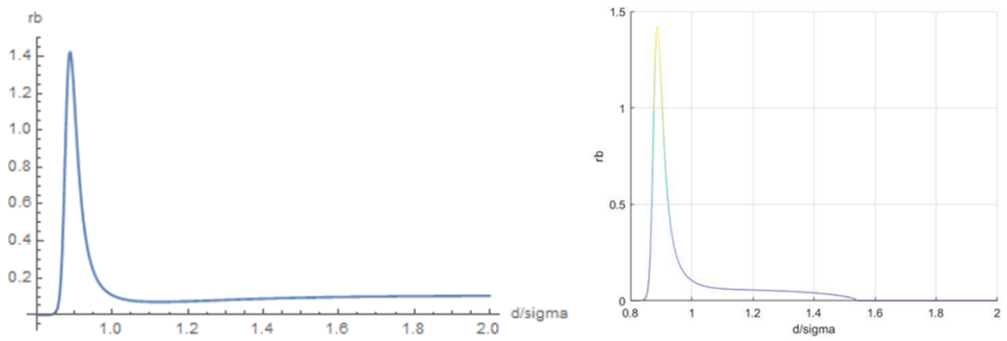

Figure 16. Graph of reaction rate vs d/σ at T= 600K based on two models at φ_s/k=-7500, ε/k=250, E_0/k=2000, K_0=3, Z=1, X_b=0.001, the left one is based on the two-site model including non-mean field terms and the right one is based on two-site model considering $P_{collision}$

As shown in Figure 16, our previous model has an apparent problem that when d/σ keeps increasing, the reaction rate keeps going on at large d/σ value which does not make any sense. The main problem for the previous model is that it does not consider the kinetic energy owned by each molecule. Even though the molecules are attached to the active sites, they are still under vibration.

In the latest model, we incorporated the parameter about probability of hitting which greatly resolves the problem above and Figure 13 shows the relationship between reaction rate, d/σ values and temperature. Figure 14 tells us that the reaction rate does reach its peak at a certain temperature, and Figure 15 indicates that the reaction rate also reaches its peak at a certain d/σ value. In addition, the result of Figure 15 indicates a certain distance over which leads to no reaction and the threshold distances increases with temperature increases. This phenomenon is easy to be comprehended since higher temperature gives molecules bigger kinetic energy to overcome the potential energy, and therefore the movement amplitude of each molecule becomes larger.

3, Experiments on Measuring Adsorption Isotherms

a) General Design of Our Experiments

Our experiment used Autochem 2920 connected with a mass spectroscopy (MS) machine to measure the adsorption amount of CO on 0.1g of HZSM-5 at 35 °C. We used the values from MS instead of TCD because TCD values also incorporated many other impurities, such as water and carbon dioxide. To perform the experiment, initially, we baked our sample to remove the molecules on its surface. Then, we let CO/He stream at 35 °C to let the surface of zeolite saturated with CO that it could adsorbed. Next, we changed the CO/He mixture to pure helium to remove the physiosorbed gas. After that, we reheated our sample to 500 °C to remove the chemisorbed gas and then went back to 35 °C.

b) Gradual Modification on the Experimental Procedure

Since nobody has done experiments like us before, all the procedures need to be testified and corrected to make sure that all the data we got were accurate. The first modification we did was to determine and calculate physisorption and chemisorption area. As shown in Figure 17, we used the area of the shaded region on the MS graph to be the physisorption amount during our experiments, where the starting points is the first inflection point on the graph. In Figure 18, we used the area of the shaded region on the MS graph to be the chemisorption amount. The base line could be found after the huge water peak.

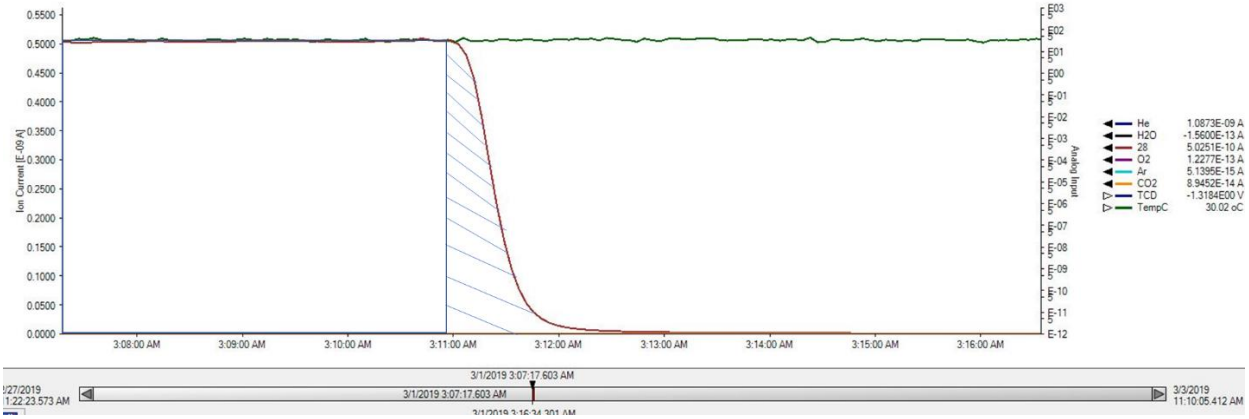

Figure 17. A sample graph showing the calculation of physisorption amount

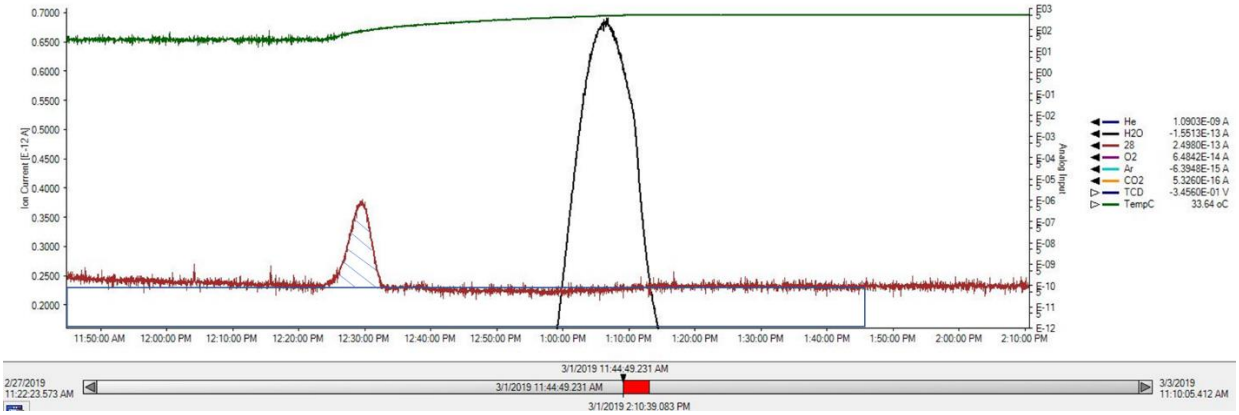

Figure 18. A sample graph showing the calculation of chemisorption amount

To get accurate data and find the relationship between gas concentration and adsorption amount, another important point is that the sample needs to be the same throughout the experiment. Since the sample may have some reactions with the CO gas and the sample itself may contain a lot of impurities inside. Therefore, initially we baked out all the water and impurities inside and then repeated the same experiments for several times until the area of both physisorption and chemisorption approached the same. From the Figure 19 and 20, we found that the impurity amount was very low and both the physisorption and the chemisorption graph were almost the same from the fourth to the sixth experiment, which means that the system had achieved balance.

After several experiments, we determined that 800 °C is high enough to pretreat the sample and six times of repeat are long enough for the systems to achieve balance.

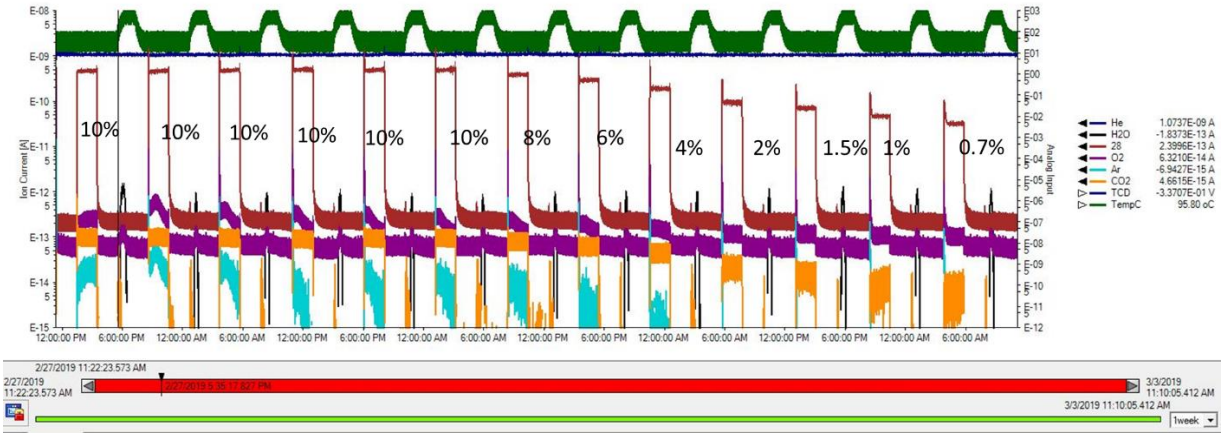

Figure 19. MS graph for the CO adsorption from 0.7% to 10%

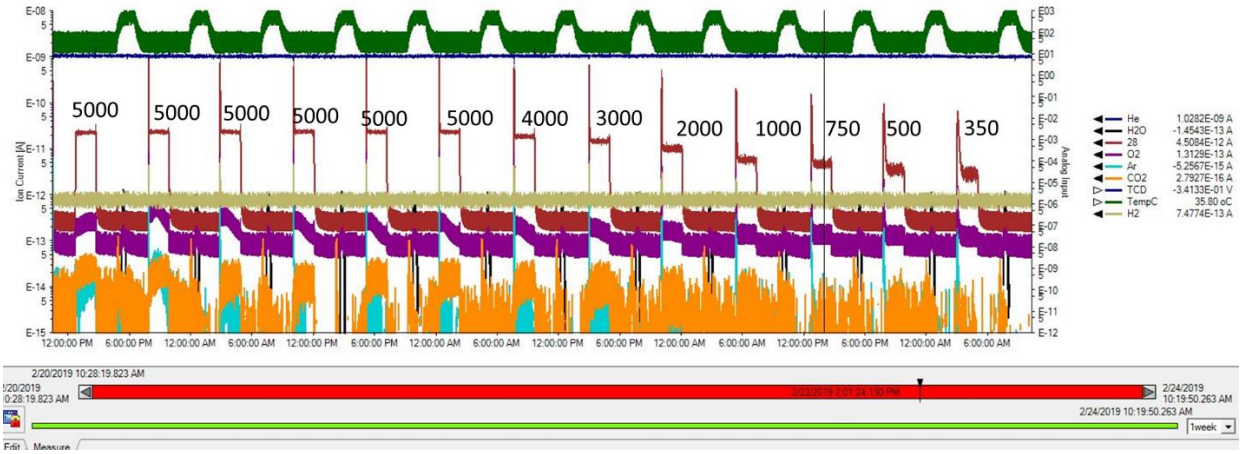

Figure 20. MS graph for the CO adsorption from 350 ppm to 5000 ppm

In addition, the determination of the physisorption time is also an important consideration in this experiment. If the waiting time is too short, the physisorption line will not reach equilibrium, and the physisorption value we calculate will have no meaning. If the waiting time is too long, the whole experiment will take a lot more time and decrease the efficiency. Therefore, finding an

appropriate waiting time is very important in this experiment. After massive explorations, we found several interesting phenomena. First, higher concentration of CO gas is much easier to get stable line. Also, higher percentage of carrier gas (pure He) is much easier to get stable line and inert gas (like Ar) reaches stable line very fast. In Table 1, we summarized the optimal waiting time to reach equilibrium for different kinds of gases.

Table 1. Waiting time for different types of gases

Gas tank type	Actual gas concentration	Time
10% nitrogen	0.7-10%	2 hr
10%Ar	0.7-10%	2 hr
10% CO	0.7-10%	2 hr
5000 ppm CO	350-5000 ppm	2 hr
500 ppm CO	300-500 ppm	5 hr
500 ppm CO	35-200 ppm	2 hr
50 ppm CO	30-50 ppm	7 hr
50 ppm CO	3.5-20	3.5 hr

The last important point that we kept modifying is how to get a series of data. Since the lowest gas concentration allowed by Autochem 2920 for a certain concentration of gas tank is about 0.07 of the marked concentration on the gas tank, we need to use several different gas tanks to

measure the adsorption isotherm over a wide concentration range. To solve this problem, we decided to buy gas tanks of 50 ppm CO, 500 ppm CO, 5000 ppm CO and 10% CO to make sure that we could measure the adsorption amount at any point from 3.5 ppm to 10%, which is a large enough range for the project. For every gas tank, we picked up eight points in its region. They were 0.07, 0.1, 0.15, 0.2, 0.4, 0.6, 0.8, 1 of the mark value. We selected these eight points to consider both adsorption versus concentration and adsorption versus ln (concentration) cases. Initially, we just measured a series of data using one sample, then changed for another sample and repeated the experiment in a different concentration region. However, we found that the size of the sample granules was not evenly distributed. To ensure accuracy of the experiment, the same sample should be used for all the measurements and the experiment procedures need to have some modification. Therefore, once we need to switch to another gas tank, we manually closed all the valves connected to the gas tank first to prevent large amount of gases moved into the sample. After connecting to the new gas tank, we did not bake the sample again to prevent any reaction associated with temperature. We just used carrier gas to flush the system for six hours to remove anything inside the sample and then began the next measurement.

(c) Results and Discussion

(a)

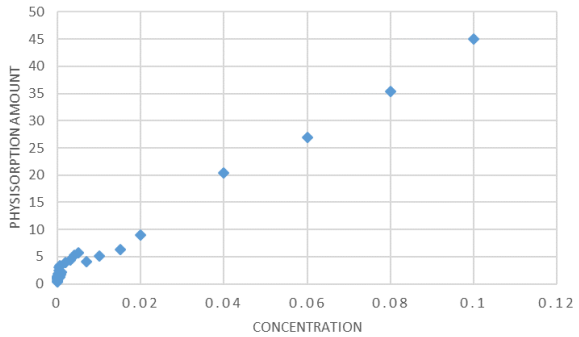

(b)

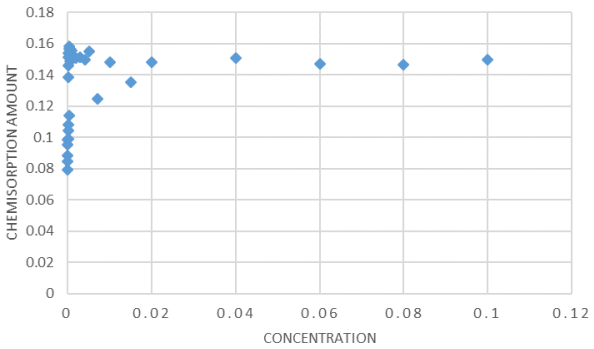

(c)

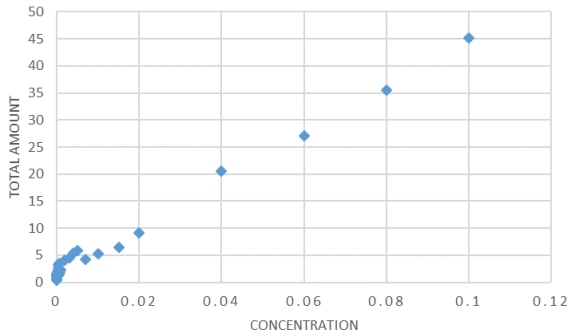

Figure 21. Adsorption amount vs concentration for CO, where (a) is physisorption, (b) is chemisorption and (c) is total adsorption

(a)

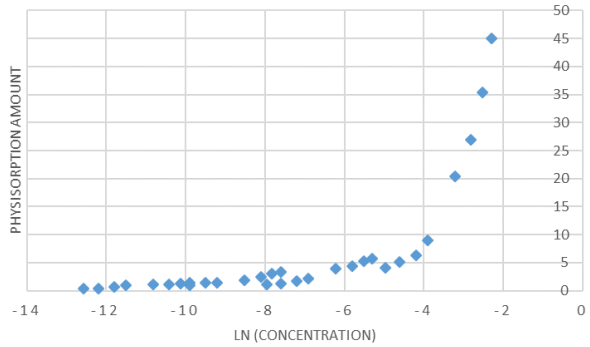

(b)

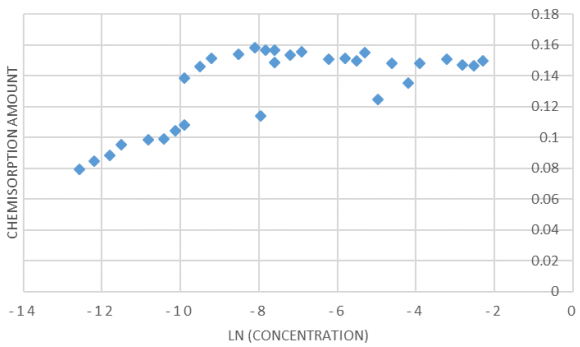

(c)

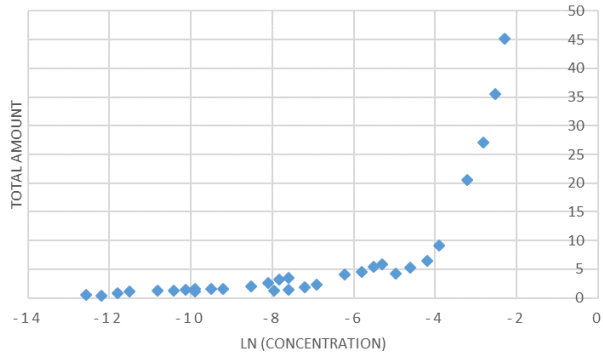

Figure 22. Adsorption amount vs ln (concentration) for CO, where (a) is physisorption, (b) is chemisorption and (c) is total adsorption

(a)

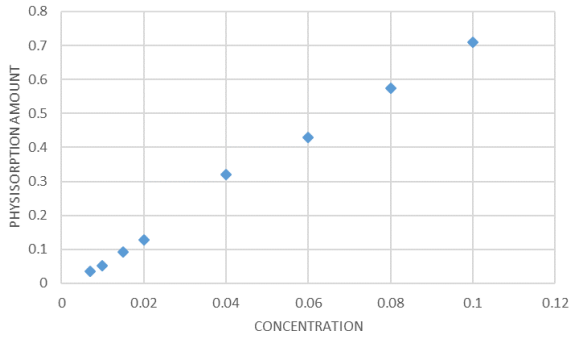

(b)

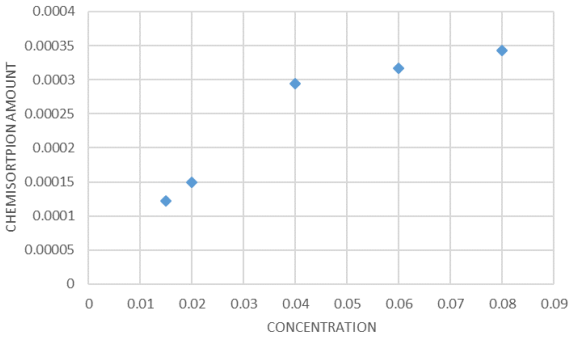

(c)

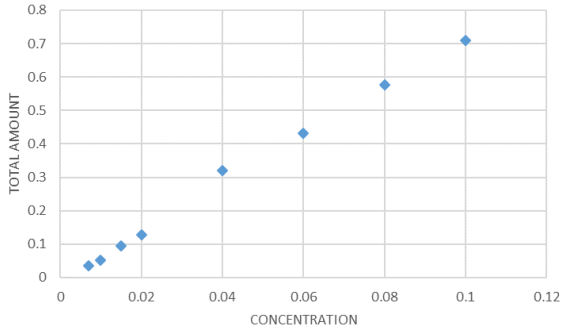

Figure 23. Adsorption amount vs concentration for N_2, where (a) is physisorption, (b) is chemisorption and (c) is total adsorption

(a) (b)

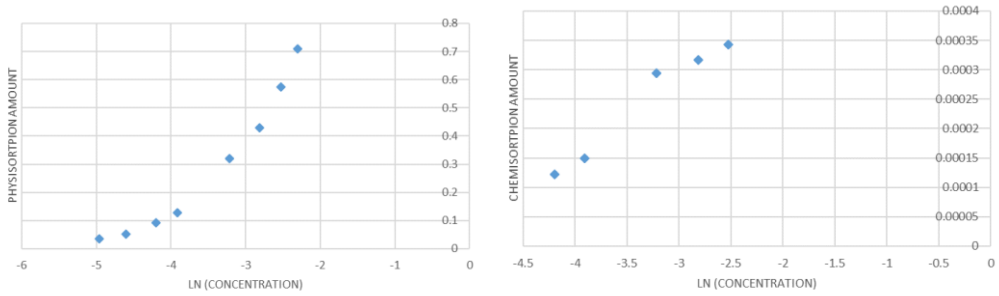

(c)

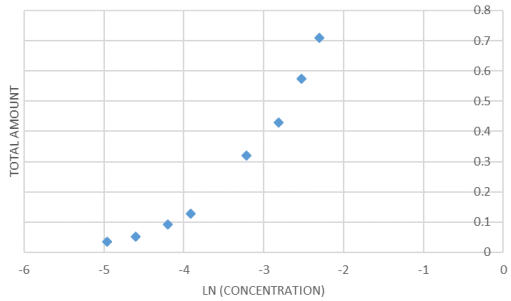

Figure 24. Adsorption amount vs ln (concentration) for N_2, where (a) is physisorption, (b) is chemisorption and (c) is total adsorption

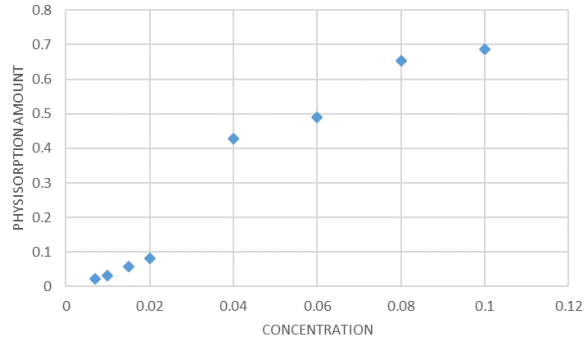

Figure 25. Physisorption adsorption amount vs concentration for Ar

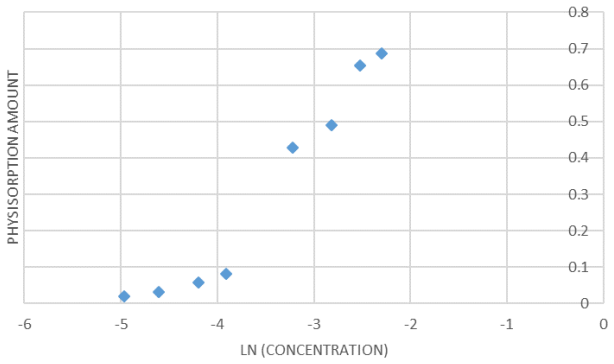

Figure 26. Physisorption adsorption amount vs ln (concentration) for Ar

The Figure 21-26 above comes from the adsorption data from Appendix 5, 6 and 7. Those figures indicate that physisorption amount dominates the total adsorption amount, especially when the gas concentration is high. Also, chemisorption does not happen for every kind of gas, especially for inert and nonpolar gas. This phenomenon is reasonable since the inert gas is difficult to form a bond to other molecules. Therefore, almost no chemisorption can be identified. However, because of the existence of London dispersion force, even inert gas will have some physical connection between gas molecules and the active sites, leading to a certain amount of physisorption.

Also, these data verify that the Langmuir's isotherm is a good approximation to physisorption isotherms at low concentration. However, when the concentration goes higher, the level off phenomenon for adsorption amount cannot be identified, and the physisorption amount has a linear relationship with concentration in this case. This phenomenon can be explained that the Langmuir's theory does not consider the lateral interaction between adsorbate molecules. At low concentration, the assumption is reasonable since the lateral interaction may be very small. However, at high concentration, we cannot overlook the influence of lateral energy and that is the reason why the Langmuir's theory is not accurate at high concentration.

Furthermore, the adsorption isotherm from the data of our chemisorption values show a huge similarity with the adsorption isotherm drawn from the Grand Canonical Model, which means that the Grand Canonical Model can be a useful tool to study chemisorption. This phenomenon can be explained that Grand Canonical Model assumes a strong interaction between adsorbate molecules and active sites, and chemisorption is just a kind of adsorption that forms a strong chemical bonding. Moreover, the adsorption amount increases as the molecules becomes more polar and reactive. For CO, we can have a discernible adsorption amount on HZSM-5 at room temperature.

Conclusion

Based on Grand Canonical Model, we developed three two-site models to describe the relationship between reaction rate, temperature and distances between to active sites. When d/σ is bigger than 0.90, all these three models show that for a certain distance, reaction rate increases with temperature initially and then gradually goes to 0. However, for a certain temperature, the previous two models show that the reaction rate will not go to 0 as distance keeps increasing to a nonzero number, which directly contradicts our assumption. For the last model considering the collision probability, there is a threshold distance that over such a distance, no reaction could happen, which follows our assumption. Therefore, the two-site model, which includes non-mean field terms in Arrhenius factor and collision probability in pre-exponential of the rate of reaction and adsorption isotherm, can be a perfect model to describe the relationship between reaction rate, temperature and distances.

Based on the adsorption isotherms of CO, Ar and N_2 on the surface of HZSM-5, physisorption dominates the total adsorption amount, especially for high concentration. Meanwhile, chemisorption does not happen for every kind of gas, especially for inert as well as nonpolar gas, and the adsorption amount increases as the molecules becomes more polar and reactive. For CO, we could have a discernible chemisorption amount on HZSM-5 at room temperature.

Quantitatively, physisorption at low concentration follows Langmuir's theory very well. However, when the concentration goes higher, the physisorption amount shows a linear relationship with concentration for all these gases. By contrast, the chemisorption isotherms show a huge similarity with the adsorption isotherms drawn from the Grand Canonical Model, which means that the Grand Canonical Model can be a good tool to study chemisorption

Bibliography

1. Czelej, K.; Cwieka, K.; Colmenares, J.C.; Kurzydlowski, K.J. (2016). "Insight on the Interaction of Methanol-Selective Oxidation Intermediates with Au- or/and Pd-Containing Monometallic and Bimetallic Core@Shell Catalysts". *Langmuir*. 32 (30): 7493–7502
2. Foo, K. Y.; Hameed, B. H. (2010). "Insights into the modeling of adsorption isotherm systems". *Chemical Engineering Journal*. 156 (1): 2–10
3. Langmuir, I. *J. Am. Chem. Soc.* **1916**, *38*, 2221.
4. Frumkin, A. *Z. Phys. Chem.* (Leipzig) **1925**, *116*, 466.
5. Fowler, R. H.; Guggenheim, E. A. *Statistical Thermodynamics*; Cambridge University Press: London, 1949.
6. G. L. Aranovich; M. D. Donohue. “Adsorption Compression: An Important New Aspect of Adsorption Behavior and Capillarity”. *Langmuir* 2003 19 (7), 2722-2735
7. Brunauer, S.; Emmett, P. H.; Teller, E. *J. Am. Chem. Soc.* **1938**, 60, 309
8. Ono, S.; Kondo, S. Molecular Theory of Surface Tension in Liquids. In *Encyclopedia of Physics*; Flugge, S., Ed.; Springer: Berlin, **1960**; Vol. 10, p 134.
9. Aranovich, G. L.; Donohue, M. D. *Physica A* **1997**, *242*, 409.
10. Aranovich, G. L.; Donohue, M. D. *J. Colloid Interface Sci*. **1998**, *200*, 273.
11. Aranovich, G. L.; Donohue, M. D. *Phys. Rev. E* **1999**, *60*, 5552.
12. Aranovich, G. L.; Donohue, M. D. *J. Chem. Phys*. **2000**, *112*, 2361
13. Aranovich, G. L.; Donohue, M. D. *J. Colloid Interface Sci.* **1997**, *189*, 101.
14. Donohue, M. D.; Aranovich, G. L. *J. Colloid Interface Sci.* **1998**, *205*, 121
15. Aranovich, G. L.; Donohue, M. D. *J. Chem. Phys.* **1996**, *104*, 3851.

16. Aranovich, G. L.; Donohue, M. D. *J. Colloid Interface Sci.* **1996**, *180*, 537.

17. Donohue, M. D.; Aranovich, G. L. *Adv. Colloid Interface Sci.* **1998**, *76-77*, 137.

18. Donohue, M. D.; Aranovich G. L. *Fluid Phase Equilib.* **1999**, *158*, 557

19. Israelachivill, J. *Intermolecular and Surface Forces*; Academic Press: Suffolk, 1991, p 50-52

Appendices

1. Table for Variables

Variable	Old notation	New notation	Property
number of molecules on two active sites	N	N	
chemical potential	μ	μ	usually <=0
configurational energy of two states where only one of sites is occupied	ε_s	φ_s	usually <=0
the depth of potential well	ε	ε	always positive
the interaction energy between molecules sitting on both sites/ the energy of interaction between neighbors	φ/ε	φ or $\varphi(d)$	usually <=0 if ψ=0 then it follows Langmuir's Theory
interaction energy between molecules sitting on both sides in the adsorbed layer		φ_a	$\varphi(d)=\varphi_a+\varphi_b$ with φ_b=0 in this discussion
interaction energy between molecules sitting on both sides in the bulk layer		φ_b	
distance between two active sites	d	d	
size of molecules	σ	σ	intersection point between curve and x axis
reaction rate for biomolecular reaction	R_b	R_b	

classical catalytic reaction barrier	E_0	E_0	normally positive
adsorbed coordination number	z	z_a	
bulk coordination number	z	z_b	
the reduced density of adsorbate molecules in the bulk	x_b	x_b	
adsorption isotherm	x1(xb)	$x_a(x_b)$	
double occupancy probability	P_{double}	P_{double}	
the limit of the kinetic constant at high temperature	k_0	k_0	
temperature	T	T	
scaled classical catalytic reaction barrier		E_a	$E_a=E_0/k$
collision probability		$P_{collision}$	

2. Parameters and MATLAB Code for the Inclusion of Mean Field Approximation in Arrhenius Factor of the Rate of Reaction and Adsorption Isotherm

Parameters:

μ/k=A, φs/k=B, ε/k=C, d/σ=F, E0/k=Ea (B, C, Ea should all be negative)

B=-7500, C=250, F=0.95, Ea=2000, Kzero=3, Z=4, xb=0.001

MATLAB code for r_b vs T for certain d/σ value and different x_b values

```
function rate_new
for ea=2000
es=-7500;
xb=0.001;
z=4;
kzero=3;
ep=250;
rb=[];
f=0.95;
for t=0:10:3000
    x=0.04;
    error=10000;
    while error > 1e-5
    kstar=exp(-es./t - z*ep*4*(f^(-12)-f^(-6))./t*x);
    x_new=kstar.*xb./(1+kstar.*xb);
    error=abs(x_new-x)/x;
    x=x_new;
    end
if (-ea/t)+((z*ep*4*(f^(-12)-f^(-6))/t)*x_new)<0
r=kzero*x_new^2*exp((-ea/t)+((z*ep*4*(f^(-12)-f^(-
6))/t)*x_new));
else
r=kzero*x_new^2;
end
rb=[rb,r];
end

xb_1=0.01;
rb_1=[];
for t=0:10:3000
    x_1=0.04;
    error=10000;
```

```
    while error > 1e-5
    kstar=exp(-es./t - z*ep*4*(f^(-12)-f^(-6))./t*x_1);
    x_new_1=kstar.*xb_1./(1+kstar.*xb_1);
    error=abs(x_new_1-x_1)/x_1;
    x_1=x_new_1;
    end
if (-ea/t)+((z*ep*4*(f^(-12)-f^(-6))/t)*x_new_1)<0
r_1=kzero*x_new_1^2*exp((-ea/t)+((z*ep*4*(f^(-12)-f^(-
6))/t)*x_new_1));
else
r_1=kzero*x_new_1^2;
end
rb_1=[rb_1,r_1];
end


xb_2=0.1;
rb_2=[];
for t=0:10:3000
    x_2=0.04;
    error=10000;
    while error > 1e-5
    kstar=exp(-es./t - z*ep*4*(f^(-12)-f^(-6))./t*x_2);
    x_new_2=kstar.*xb_2./(1+kstar.*xb_2);
    error=abs(x_new_2-x_2)/x_2;
    x_2=x_new_2;
    end
if (-ea/t)+((z*ep*4*(f^(-12)-f^(-6))/t)*x_new_2)<0
r_2=kzero*x_new_2^2*exp((-ea/t)+((z*ep*4*(f^(-12)-f^(-
6))/t)*x_new_2));
else
r_2=kzero*x_new_2^2;
end
rb_2=[rb_2,r_2];
end



plot(0:10:3000,rb,'color','r'); hold on;
plot(0:10:3000,rb_1,'color','b'); hold on;
plot(0:10:3000,rb_2,'color','k');


end
xlabel('Temperature/K')
ylabel('rb')
```

```
end
```

MATLAB code for r_b vs T for certain x_b value and d/σ value but different activation energies

```
function rate
ea_1=2000;
ea_2=2100;
ea_3=2200;
ea_4=2300;
es=-7500;
xb=0.001;
z=4;
kzero=3;
ep=250;
rb_1=[];
rb_2=[];
rb_3=[];
rb_4=[];
for t=20:10:1000
    x=0.04;
    error=10000;
    while error > 1e-5
    kstar=exp(-es./t - z*ep*4*(0.95^(-12)-0.95^(-6))./t*x);
    x_new=kstar.*xb./(1+kstar.*xb);
    error=abs(x_new-x)/x;
    x=x_new;
    end
if (-ea_1/t)+((z*ep*4*(0.95^(-12)-0.95^(-6)))/t)*x_new <0
r_1=kzero*x_new^2*exp((-ea_1/t)+((z*ep*4*(0.95^(-12)-0.95^(-
6)))/t)*x_new);
else
    r_1=kzero*x_new^2;
end
rb_1=[rb_1,r_1];

if (-ea_2/t)+((z*ep*4*(0.95^(-12)-0.95^(-6)))/t)*x_new<0
r_2=kzero*x_new^2*exp((-ea_2/t)+((z*ep*4*(0.95^(-12)-0.95^(-
6)))/t)*x_new);
else
r_2=kzero*x_new^2;
end
rb_2=[rb_2,r_2];
```

```
if (-ea_3/t)+((z*ep*4*(0.95^(-12)-0.95^(-6)))/t)*x_new<0
r_3=kzero*x_new^2*exp((-ea_3/t)+((z*ep*4*(0.95^(-12)-0.95^(-
6)))/t)*x_new);
else
r_3=kzero*x_new^2;
end
rb_3=[rb_3,r_3];

if (-ea_4/t)+((z*ep*4*(0.95^(-12)-0.95^(-6)))/t)*x_new<0
r_4=kzero*x_new^2*exp((-ea_4/t)+((z*ep*4*(0.95^(-12)-0.95^(-
6)))/t)*x_new);
else
r_4=kzero*x_new^2;
end
rb_4=[rb_4,r_4];
end
plot(20:10:1000,rb_1,'color','r'); hold on;
plot(20:10:1000,rb_2,'color','b'); hold on;
plot(20:10:1000,rb_3,'color','k'); hold on;
plot(20:10:1000,rb_4,'color','g');


xlabel('Temperature/K')
ylabel('rb')


end
```

MATLAB code for r_b vs T for certain X_b value and activation energies but different d/σ values

```
function rate_new
for ea=2000
es=-7500;
xb=0.001;
z=4;
kzero=3;
ep=250;
rb=[];
f=0.95;
for t=0:10:3000
    x=0.04;
    error=10000;
    while error > 1e-5
```

```
    kstar=exp(-es./t - z*ep*4*(f^(-12)-f^(-6))./t*x);
    x_new=kstar.*xb./(1+kstar.*xb);
    error=abs(x_new-x)/x;
    x=x_new;
    end
if (-ea/t)+((z*ep*4*(f^(-12)-f^(-6))/t)*x_new)<0
r=kzero*x_new^2*exp((-ea/t)+((z*ep*4*(f^(-12)-f^(-
6))/t)*x_new));
else
r=kzero*x_new^2;
end
rb=[rb,r];
end

xb_1=0.001;
rb_1=[];
f_1=1.05;
for t=0:10:3000
    x_1=0.04;
    error=10000;
    while error > 1e-5
    kstar=exp(-es./t - z*ep*4*(f_1^(-12)-f_1^(-6))./t*x_1);
    x_new_1=kstar.*xb_1./(1+kstar.*xb_1);
    error=abs(x_new_1-x_1)/x_1;
    x_1=x_new_1;
    end
if (-ea/t)+((z*ep*4*(f_1^(-12)-f_1^(-6))/t)*x_new_1)<0
r_1=kzero*x_new_1^2*exp((-ea/t)+((z*ep*4*(f_1^(-12)-f_1^(-
6))/t)*x_new_1));
else
r_1=kzero*x_new_1^2;
end
rb_1=[rb_1,r_1];
end


xb_2=0.001;
rb_2=[];
f_2=1.5;
for t=0:10:3000
    x_2=0.04;
    error=10000;
    while error > 1e-5
    kstar=exp(-es./t - z*ep*4*(f_2^(-12)-f_2^(-6))./t*x_2);
    x_new_2=kstar.*xb_2./(1+kstar.*xb_2);
    error=abs(x_new_2-x_2)/x_2;
    x_2=x_new_2;
```

```
    end
if (-ea/t)+((z*ep*4*(f_2^(-12)-f_2^(-6))/t)*x_new_2)<0
r_2=kzero*x_new_2^2*exp((-ea/t)+((z*ep*4*(f_2^(-12)-f_2^(-
6))/t)*x_new_2));
else
r_2=kzero*x_new_2^2;
end
rb_2=[rb_2,r_2];
end

xb_3=0.001;
rb_3=[];
f_3=10000;
for t=0:10:3000
    x_3=0.04;
    error=10000;
    while error > 1e-5
    kstar=exp(-es./t - z*ep*4*(f_3^(-12)-f_3^(-6))./t*x_2);
    x_new_3=kstar.*xb_3./(1+kstar.*xb_3);
    error=abs(x_new_3-x_3)/x_3;
    x_3=x_new_3;
    end
if (-ea/t)+((z*ep*4*(f_3^(-12)-f_3^(-6))/t)*x_new_3)<0
r_3=kzero*x_new_3^2*exp((-ea/t)+((z*ep*4*(f_3^(-12)-f_3^(-
6))/t)*x_new_3));
else
r_3=kzero*x_new_3^2;
end
rb_3=[rb_3,r_3];
end

plot(0:10:3000,rb,'color','r'); hold on;
plot(0:10:3000,rb_1,'color','b'); hold on;
plot(0:10:3000,rb_2,'color','k'); hold on
plot(0:10:3000,rb_3,'color','g');


end
xlabel('Temperature/K')
ylabel('rb')


end
```

3. Parameters and Mathematica Code to Calculate Reaction Rate Considering Non-mean Field Terms

Parameters

$\mu/k=A$, $\varphi_s/k=B$, $\varepsilon/k=C$, $d/\sigma=G$ $E_0/k=Ea$

Assumption: $B=-7500$; $C=250$; $E_a=2000$; $K_0=3$; $Z=1$; $X_b=0.001$

Mathematica Code for 3D plot

```
z=1
k0=3
b=-7500
c=250
ea=2000
xb=0.001
e0overkt=ea/t
miuoverkt=Log[xb]
faisoverkt=b/t
f1=Exp[miuoverkt-faisoverkt]
faioverkt=4*c/t*(g^(-12)-g^(-6))
f2=Exp[2*miuoverkt-2*faisoverkt-faioverkt]
p=f2/(2*f1+f2+1)
arr=-e0overkt+z*faioverkt*p
arr1=If[arr<0,arr,0]
rb=k0*Exp[arr1]*p
Plot3D[{rb},{t,100,1500},{g,0.80,2},AxesLabel->{"temp/k","d/sigma","rb"},PlotRange->All]
```

4. Parameters and MATLAB Code for New two-site Model Including Collision Probability in Pre-exponential of the Rate of Reaction and Adsorption Isotherm

Parameters

μ/k=A, φs/k=B, ε/k=C, d/σ=G

Assumption: B=-7500, G= 1.2, T=500

MATLAB Code for 3D plot reaction rate vs temperature vs d/σ

```
function model

num_psi = 1000;
num_iter = 300;
t_list = linspace(20,1500,num_iter);
g_list = linspace(0.8,3.0,num_iter);
rb_list = zeros(1, num_iter * num_iter);

X = zeros(1, num_iter * num_iter);
Y = zeros(1, num_iter * num_iter);

row_list = 1:num_iter;
col_list = 1:num_iter;


for count=1:num_iter*num_iter
    t = t_list(floor((count-1) / num_iter) + 1);
    g = g_list(mod((count-1), num_iter) + 1);

    b=-7500;
    c=250;
    ea=2000;
    kzero=3;
    z=1;
    xb=0.001;
    e0overkt = ea./t;
    miuoverkt = log(xb);
    faisoverkt = b./t;
    f1 = exp(miuoverkt - faisoverkt);
    faioverkt = 4*c/t*((g)^(-12) - (g)^(-6));
    f2 = exp(2*miuoverkt - 2*faisoverkt - faioverkt);
    p = f2/(2*f1 + f2 + 1);
```

```
    n=0;

    ind = 1;
    for psi=linspace(0,2*pi,num_psi)
        a=sin(psi./2)-sin(-psi./2);
        C=1-(3*t./2./b+1)^2;
        D=abs(3*t./b+2)./C^0.5*(g-1);
        y=a-D;
        if y>=0
             n=n+1;
        else
             n=n;
        end
        pr=n./num_psi;
        ind = ind + 1;
    end
    X(count) = t;
    Y(count) = g;
    if -e0overkt + z*faioverkt*p <0
    rb_list(count) = kzero*exp(-e0overkt + z*faioverkt*p)*p*pr;
    else
    rb_list(count) = kzero*p*pr;
    end
end


[xx,yy] = meshgrid(t_list,g_list);
mesh(xx,yy,reshape(rb_list, num_iter, num_iter))

xlabel('Temperature/K')
ylabel('d/sigma')
zlabel('rb')



end
```

MATLAB code for 2D plot reaction rate vs temperature at certain d/σ

```
function model

num_psi = 1000;
num_iter = 300;
t_list = linspace(200,2000,num_iter);
g_list = linspace(1.25,1.25,num_iter);
```

```
rb_list = zeros(1, num_iter * num_iter);

X = zeros(1, num_iter * num_iter);
Y = zeros(1, num_iter * num_iter);

row_list = 1:num_iter;
col_list = 1:num_iter;


for count=1:num_iter*num_iter
    t = t_list(floor((count-1) / num_iter) + 1);
    g = g_list(mod((count-1), num_iter) + 1);

    b=-7500;
    c=250;
    ea=2000;
    kzero=3;
    z=1;
    xb=0.001;
    e0overkt = ea./t;
    miuoverkt = log(xb);
    faisoverkt = b./t;
    f1 = exp(miuoverkt - faisoverkt);
    faioverkt = 4*c/t*((g)^(-12) - (g)^(-6));
    f2 = exp(2*miuoverkt - 2*faisoverkt - faioverkt);
    p = f2/(2*f1 + f2 + 1);
    n=0;

    ind = 1;
    for psi=linspace(0,2*pi,num_psi)
        a=sin(psi./2)-sin(-psi./2);
        C=1-(3*t./2./b+1)^2;
        D=abs(3*t./b+2)./C^0.5*(g-1);
        y=a-D;
        if y>=0
             n=n+1;
        else
             n=n;
        end
        pr=n./num_psi;
        ind = ind + 1;
    end
    X(count) = t;
    Y(count) = g;
        if -e0overkt + z*faioverkt*p <0
    rb_list(count) = kzero*exp(-e0overkt + z*faioverkt*p)*p*pr;
    else
```

```
    rb_list(count) = kzero*p*pr;
        end
end


[xx,yy] = meshgrid(t_list,g_list);
mesh(xx,yy,reshape(rb_list, num_iter, num_iter))


xlabel('temperature/K')
ylabel('d/sigma')
zlabel('rb')
end
```

MATLAB Code for 2D plot reaction rate vs d/σ at certain T

```
function model

num_psi = 1000;
num_iter = 300;
t_list = linspace(600,600,num_iter);
g_list = linspace(0.8,2,num_iter);
rb_list = zeros(1, num_iter * num_iter);

X = zeros(1, num_iter * num_iter);
Y = zeros(1, num_iter * num_iter);

row_list = 1:num_iter;
col_list = 1:num_iter;


for count=1:num_iter*num_iter
    t = t_list(floor((count-1) / num_iter) + 1);
    g = g_list(mod((count-1), num_iter) + 1);

    b=-7500;
    c=250;
    ea=2000;
    kzero=3;
    z=1;
    xb=0.001;
    e0overkt = ea./t;
    miuoverkt = log(xb);
    faisoverkt = b./t;
    f1 = exp(miuoverkt - faisoverkt);
```

```
    faioverkt = 4*c/t*((g)^(-12) - (g)^(-6));
    f2 = exp(2*miuoverkt - 2*faisoverkt - faioverkt);
    p = f2/(2*f1 + f2 + 1);
    n=0;

    ind = 1;
    for psi=linspace(0,2*pi,num_psi)
        a=sin(psi./2)-sin(-psi./2);
        C=1-(3*t./2./b+1)^2;
        D=abs(3*t./b+2)./C^0.5*(g-1);
        y=a-D;
        if y>=0
             n=n+1;
        else
             n=n;
        end
        pr=n./num_psi;
        ind = ind + 1;
    end
    X(count) = t;
    Y(count) = g;
        if -e0overkt + z*faioverkt*p <0
    rb_list(count) = kzero*exp(-e0overkt + z*faioverkt*p)*p*pr;
    else
    rb_list(count) = kzero*p*pr;
        end
end


[xx,yy] = meshgrid(t_list,g_list);
mesh(xx,yy,reshape(rb_list, num_iter, num_iter))


xlabel('temperature/K')
ylabel('d/sigma')
zlabel('rb')
end
```

5. Adsorption data for CO on HZSM-5

Concentration	Ln C	Physisorption	Chemisorption	Total
100000 ppm	-2.30259	44.94915	0.149762	45.09891
80000 ppm	-2.52573	35.37	0.146389	35.51639
60000 ppm	-2.81341	26.9746	0.146953	27.12156
40000 ppm	-3.21888	20.46154	0.150811	20.61235
20000 ppm	-3.91202	8.972222	0.147955	9.120177
15000 ppm	-4.19971	6.249057	0.135333	6.38439
10000 ppm	-4.60517	5.050746	0.148235	5.198982
7000 ppm	-4.96185	4.1448	0.124444	4.269244
5000 ppm	-5.29832	5.75	0.155	5.905
4000 ppm	-5.52146	5.285714	0.15	5.435714
3000 ppm	-5.80914	4.421053	0.151579	4.572632
2000 ppm	-6.21461	3.893478	0.150915	4.044393
1000 ppm	-6.90776	2.097917	0.155676	2.253592
750 ppm	-7.19544	1.639024	0.153459	1.792484
500 ppm	-7.6009	1.209756	0.148571	1.358328
350 ppm	-7.95758	1.090909	0.114073	1.204982
500 ppm	-7.60090246	3.347826	0.156471	3.504297
400 ppm	-7.824046011	2.984211	0.156522	3.140732
300 ppm	-8.111728083	2.418	0.158211	2.576211

200 ppm	-8.517193191	1.86	0.15381	2.01381
100 ppm	-9.210340372	1.477234	0.151188	1.628422
75 ppm	-9.498022444	1.43	0.146051	1.576051
50 ppm	-9.903487553	1.367273	0.138444	1.505717
35 ppm	-10.2601625	1.16	0.111176	1.271176
50 ppm	-9.90349	0.9855	0.09375	1.0245
40 ppm	-10.1266	1.243478	0.094706	1.338184
30 ppm	-10.4143	1.174468	0.093714	1.966055
20 ppm	-10.8198	1.171852	0.0658	1.237652
10 ppm	-11.5129	0.986087	0.077647	1.063734
7.5 ppm	-11.8006	0.679412	0.102857	0.782269
5 ppm	-12.2061	0.35	0.078684	0.428684
3.5 ppm	-12.5627	0.387292	0.083571	0.470863

6. Adsorption data for Argon on HZSM-5

Concentration	Ln C	Chemisorption	Physisorption
100000 ppm	-2.30259	0	0.687719
100000 ppm	-2.30259	0	0.772941
100000 ppm	-2.30259	0	0.687143
100000 ppm	-2.30259	0	0.807692
100000 ppm	-2.30259	0	0.702034
100000 ppm	-2.30259	0	0.686452
80000 ppm	-2.52573	0	0.653571
60000 ppm	-2.81341	0	0.489184
40000 ppm	-3.21888	0	0.429
20000 ppm	-3.91202	0	0.082782
15000 ppm	-4.19971	0	0.0585
10000 ppm	-4.60517	0	0.032143
7000 ppm	-4.96185	0	0.021327

7. Adsorption data for Nitrogen on HZSM-5

Concentration	Ln C	phys	chem	total
100000 ppm	-2.30259	0.7104	0.000886	0.711286
100000 ppm	-2.30259	0.757209	0.00048	0.757689
100000 ppm	-2.30259	0.757037	0.000213	0.75725
100000 ppm	-2.30259	0.757209	0.000179	0.757388
100000 ppm	-2.30259	0.714483		0.714483
100000 ppm	-2.30259	0.71		0.71
80000 ppm	-2.52573	0.575	0.000343	0.575343
60000 ppm	-2.81341	0.43037	0.000317	0.430687
40000 ppm	-3.21888	0.31961	0.000294	0.319904
20000 ppm	-3.91202	0.128333	0.00015	0.128483
15000 ppm	-4.19971	0.093538	0.000122	0.093661
10000 ppm	-4.60517	0.050885		0.050885
7000 ppm	-4.96185	0.036281		0.036281

Curriculum Vitae

Ruiyang Zhao

Date of Birth: 05/20/1993
Birthplace: Nanjing, Jiangsu, China
Address: 3501 Saint Paul Street Apt 1037, Baltimore, MD, 21218
Phone: (706)-231-8188 E-mail: ruiyangzhao@hotmail.com

EDUCATION

Johns Hopkins University, Baltimore, MD 08/2017-Present

- Master of Science, Chemical Engineering

Overall GPA: 3.8 /4.0

Georgia Institute of Technology, Atlanta, GA 08/2011-05/2016

- Bachelor of Science, Chemical Engineering (minor: Japanese)

Overall GPA: 3.5/4.0

Tokyo Institute of Technology, Tokyo, Japan 03-08/2015

- Exchange student, Laboratory for Chemistry & Life Science Institute of Innovative Research

RESEARCH EXPERIENCE

Adsorption Compression, directed by Marc D. Donohue, Johns Hopkins University 12/2017-05/2019

- Studied a universal catalytic mechanism
- Established two-site models based on different assumptions to describe the adsorption isotherms and to predict reaction rates
- Measured the adsorption isotherms for various gases by using AutoChem 2920 and compared the experiment results to my models

Colloids, Polymer and Interfacial Science, directed by Dr. Sven Behrens, Georgia Tech 08/2014-05/2016

Project I: Capillary foams

- Probed into the formation stages, stabilization mechanism, and application for a new type of foam material called capillary foams
- Explored the methods to synthesize high-strength, lightweight polymeric foam materials with intense coloration
- Investigated the flow behavior of capillary foams in a porous environment for enhanced oil recovery in depth

Project II: Cellulose particles, a novel wetting modifier in colloidal multiphase systems

- Researched the wetting behavior for cellulose particles, and demonstrated that cellulose particles can be used as environment-friendly, highly harsh-condition-tolerant wetting modifiers for the cleaning
- Evaluated interfacial activities, such as surface tension and packing behavior, of colloidal particles
- Experimentally proved the validity of a new formula which accurately predicts the particle packing density based on effective interfacial tension

Polymer Electrolyte Fuel Cells, directed by Takeo Yamaguchi, Tokyo Institute of Technology 03-08/2015

- Delved into the basic principles, assembly, operations and performance analysis for PEFC
- Tested and demonstrated that increasing the membranes' permeability and decreasing the thickness of membranes are two effective ways to improve the efficiency of fuel cells

WORK EXPERIENCE

CRRC MA Corporation, Quincy, MA 05-08/2018

- Design Engineer for Heat, Ventilation and Air Conditioner System (HVAC) of the Boston Orange Metro Line
- Calculated the power needed for air conditioner and the size and shape for air ducts.
- Improved and modified airduct design and process
- Organized and instructed technicians on modification of the new airduct production line

BASF-YPC Company Limited, Nanjing, China 06-08/2013

- Process engineer in the department of ethylene synthesis
- Inquired into the principles and processes for ethylene production; practiced the operation and monitoring of ethylene production facilities; learned the problem-solving skills and safety measures used in the production of ethylene
- Made a new proposal for disposal treatment, such as Na_2S, after the caustic washing tower for environmental protection

AWARDS

- **2nd Year MSE Scholarships** issued by Whiting School of Engineering of the Johns Hopkins University (2018)

- **President's Undergraduate Research Awards** (PURA Scholarship) issued by Georgia Tech (2016)

- **Best Research Poster Award** in 2016 ChBE Air Products Undergraduate Research Symposium issued by School of Chemical and Bimolecular Engineering of Georgia Tech and Air Products & Chemicals, Inc. (2016)

- **Exchange Student Scholarship** (JASSO) issued by the Ministry of Education, Culture, Sports, Science and Technology of Japan (Japanese Government) for outstanding young research scientists (2015)

PUBLICATIONS

- Zhang, Y., Wang, S., Zhou, J., **Zhao, R.**, Benz, G., Tcheimou, S., ... & Behrens, S. H. (2017). Interfacial Activity of Nonamphiphilic Particles in Fluid–Fluid Interfaces. *Langmuir*, 33(18), 4511-4519.

- Zhang, Y., Wang, S., Zhou, J., Benz, G., Tcheimou, S., **Zhao, R.**, ... & Meredith, J. C. (2017). Capillary foams: formation stages and effects of system parameters. *Industrial & Engineering Chemistry Research*, *56*(34), 9533-9540.

- Zhang, Y., Allen, M. C., **Zhao, R.**, Deheyn, D. D., Behrens, S. H., & Meredith, J. C. (2015). Capillary foams: stabilization and functionalization of porous liquids and solids. *Langmuir*, 31(9), 2669-2676.

PRESENTATIONS

- **R. Zhao**, Y. Zhang, J. C. Meredith, S. H. Behrens, *A new method to determine the packing density of particles in fluid-fluid interfaces*, The ChBE Air Products Undergraduate Research Symposium, Atlanta, GA, 2016.

- **R. Zhao**, Y. Zhang, J. C. Meredith, S. H. Behrens, *Packing behavior of particles in fluid-fluid interfaces*, 11th Annual Undergraduate Research Symposium, Atlanta, GA, 2016.

SKILLS

- **Computer Skills**: Aspen Plus, Matlab, Microsoft Office, Mathematica, Photoshop
- **Languages**: Mandarin Chinese (native), English (bilingual proficiency), Japanese (advanced)